Bimolecular reactions of the dications and trications of atoms and small molecules in the gas-phase

Stephen D Price,* James D Fletcher, Felicity E Gossan and Michael A Parkes

Department of Chemistry, University College London, 20 Gordon Street, London WC1H 0AJ, UK

Abstract

This review discusses the recent developments in our understanding of the electron transfer and bond-forming reactions of small atomic and molecular dications in the gas-phase. A summary of the properties of isolated dications is presented, followed by a review of the major experimental techniques used to probe dicationic reactivity. Electron transfer reactions of dications with neutral species are then discussed, including recent rationalizations of this class of reactivity using simple electrostatic models. Our current understanding of the reactions of dications with neutral atoms and molecules which result in the formation of new chemical bonds is then presented. This part of the account is built around three case studies, including some new results on the bond-forming reactions of O_2^{2+} with CH_4. Moving beyond dicationic species, the account then discusses recent results concerning the bond-forming reactivity of tricationic atoms and small molecules. This section includes the mechanistic conclusions drawn from the first results involving the coincident detection of all three positively charged species generated from the reaction of a molecular trication: $CS_2^{3+} + O_2 \rightarrow SO^+ + CS^+ + O^+$. The review concludes with some thoughts concerning the future development of the field.

* corresponding author, email s.d.price@ucl.ac.uk

1. Introduction

It is well-established that the bimolecular chemistry of gas-phase monocations is crucial in determining the composition of a wide variety of media.[1-9] Perhaps most notably, the barrierless nature of many monocation–neutral reactions, which allows them to proceed efficiently at very low temperatures, allows this chemistry to make a major contribution to molecular synthesis in the cold and tenuous environment of the interstellar medium.[10] However, monocation chemistry is also important in venues as varied as planetary ionospheres,[11] etching plasmas,[12] cometary coma[13] and gas discharges.[9] Experimental investigations of gas-phase monocation-neutral chemistry, to explore and characterize these encounters, were stimulated by the recognition of the importance of this class of reactions in the media listed above. This drive to understand and document what came to be called "ion chemistry" involved the development of several important experimental techniques.[14,15] Indeed, some of these experimental techniques, for example the selected-ion flow tube (SIFT), have proven so valuable that they have become close to ubiquitous in laboratories investigating ion chemistry.[16] The reactivity data resulting from experimental studies of monocation-neutral chemistry are often rationalized using potential energy surfaces and monocation structures generated by computational initiatives.[17] This dual computational and experimental approach, has allowed complex networks of ion-molecule reactions to be constructed to explain the observed composition of, for example, interstellar clouds[1] and Titan's ionosphere.[18]

The dipositive ions of atomic and molecular species (dications) were first detected and identified early in the last century,[19-21] during the development of mass spectrometry. Later, beginning in the 1960s, a sustained campaign of experimental work began to reveal the unusual physical properties of molecular dications.[22] These unusual properties, described below, make small molecular dications very different chemical entities from molecular monocations: for example, most electronic states of small molecular dications are extremely short-lived.[23-26] Partly as a result of these unusual physical properties, it has only been in the last 20 years that experimental attention has focussed on the bimolecular reactivity of these multiply-charged species.[15,26-30] This focus was partly stimulated by modelling studies indicating that, in planetary ionospheres, molecular dications could possess comparable abundances to chemically significant monocations.[31-36]

This review focusses on our understanding of the bimolecular chemistry of atomic and small molecular dications. This focus is unashamedly experimental, highlighting the technical developments which have revealed the unusual chemistry of these high-energy species. Indeed, it is worth remarking that the pair of charges associated with dicationic systems has allowed the development of a wide range of powerful coincidence experiments to study their physical and chemical properties.[37-41] Due to their lower charge state, the range of coincidence experiments that can be applied to monocationic systems is more limited. Of course, the detailed interpretation of many of the experimental results concerning dicationic chemistry is immeasurably enhanced by the involvement of modern computational chemistry, and the value of these contributions will also be highlighted below.

This article focusses on the gas-phase reactivity of small molecular dications and trications, species composed of just a few atoms. In recent years there has been an upsurge of interest in collisions and reactions of the multiply-charged ions of large molecular species, such as biomolecules. This interest has been driven by the ease of generating such species using electrospray mass spectrometry. In such large molecules, the multiple charges can be well-separated spatially, dramatically reducing the destabilizing effect of the Coulomb repulsion. Thus, multiply-charged ions of large species display a very different chemistry to that of small multiply charged ions.[42]

It is appropriate to begin a discussion of the chemistry of small dications with a brief review of the properties of isolated dications. This account will then move on to a discussion of a number of prototypical dication-neutral reactions, highlighting the different experimental approaches that have been used to probe the chemistry of these short-lived species. Finally, the prospects for the extension of these experimental techniques to study the chemistry of cations in triply (or higher) charged states will be considered.

2. The properties of isolated dications

In a collision-free environment, such as the gas-phase, atomic dications are stable species with an electronic structure, in general, well established by atomic spectroscopy.[43] The formation of atomic dications from neutral atoms, by photoionization, generating a dication and a pair of electrons, provides a fundamental example of a "three-body problem". For this reason, the dynamics of single photon double ionization, particularly near threshold, has been extensively investigated.[44-46] When employing photoionization, the yields of multiply-charged ions are often significantly enhanced if the photon energy coincides with a resonance (e.g. the excitation of a core electron) of the neutral species, or when the photon energy can directly expel a core electron.[47-50] This study of the formation and decay of core-excited and core-ionized species has spawned a whole series of sophisticated coincidence experiments.[51] More generally, away from resonances and above the double ionization threshold, the probability for forming atomic dications is commonly of the order of a few percent with respect to that for forming a monocation.[52-54] Whereas, the yield of ions resulting from molecular double ionization (see below) is often markedly larger.[53,55-66] The technical simplicity of electron ionization sources means that electron-neutral collisions are often employed when generating multiply-charged ions for collisional experiments. [26,30,53] However, for experiments where greater control of the electronic state distribution of the reactant dication is required, ion sources using photoionization (with synchrotron radiation often providing the necessary tunability) have been developed.[67]

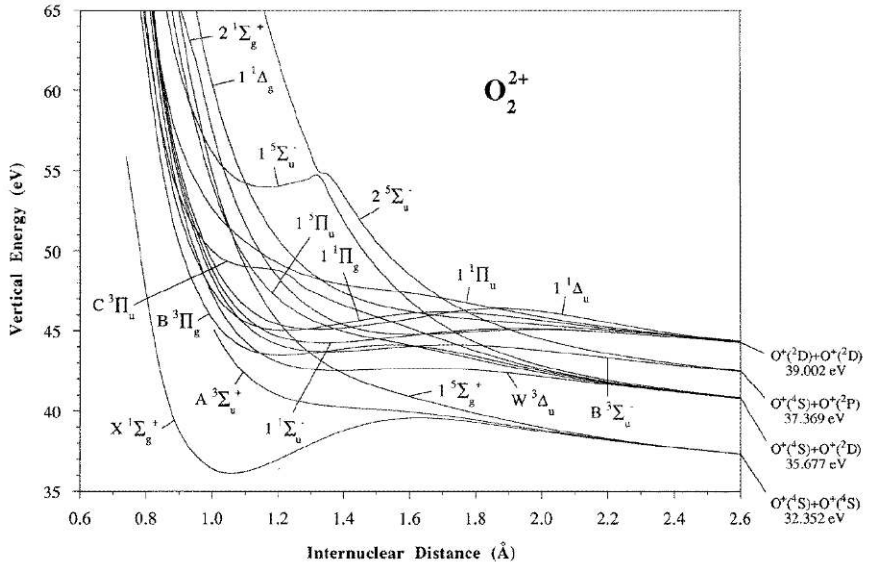

Figure 1 Potential energy curves from a series of CASSCF-MRCI calculations on O_2^{2+}. The zero point of the vertical energy scale refers to the ground state of the neutral molecules. The energy levels for the separated ion products are indicated to the right.[68]

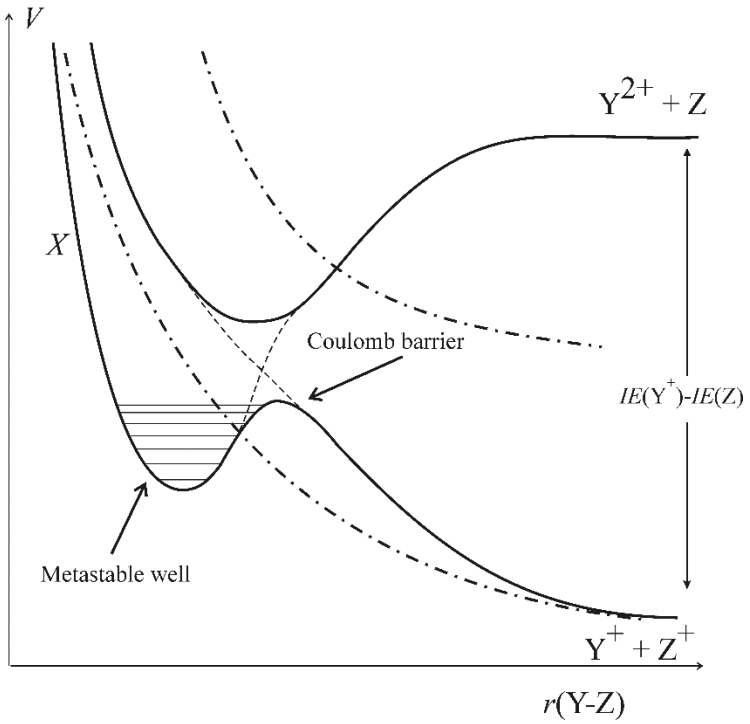

Figure 2 Schematic potentials for a diatomic dication. An avoided crossing between diabatic potentials (dashed) leads to the formation of a metastable electronic state (solid line) trapped behind a Coulomb barrier. Curve crossings to purely dissociative states (dot-dash) can provide a route for the dissociation of low lying metastable vibronic states. The energy separation between the dication-neutral and charge-separated asymptotes is equal to the difference between the second ionization energy of Y, *IE*(Y^+), and the first ionization energy of Z, *IE*(Z). See text for details. Adapted from reference [28]

As we break a bond in a molecular monocation (e.g. CO_2^+), we move towards a dissociation asymptote involving a daughter monocation and a neutral species (e.g. CO^+ + O). Since the long-range interactions between a monocation and a neutral are normally dominated by polarization-attraction, and hence are attractive, isolated molecular monocations are usually thermodynamically stable with respect to dissociation.[69] However, the addition of an additional positive charge to this monocationic system, to form a molecular dication, changes its properties dramatically. If we consider breaking a bond in a small molecular dication, and separating the two charges, electrostatic repulsion means that, in general (but not exclusively) the electronic states of small molecular dications (e.g. CO_2^{2+}) lie at higher energies than the appropriate asymptote for the charge-separated species (e.g. $CO^+ + O^+$). That is, small molecular dications are usually thermodynamically unstable with respect to charge separation.[15,23-30] Thus, one might expect that the electrostatic repulsion resulting from placing two charges in close proximity, following the double ionization of a molecule, would result in an immediate "Coulomb explosion"; a dissociation involving charge-separation.[22,70-72] Such a simple picture of the properties of molecular dications holds a great deal of truth, and the potential energy surfaces of many electronic states of molecular dications are dominated by Coulomb repulsion and are purely repulsive in nature (Figure 1).[68] However, as we see exemplified in the case of O_2^{2+} (Figure 1), in some electronic states of molecular dications the bonding interactions can be strong enough to counteract the repulsive forces between the charges. These bonding interactions result in

an energetic barrier to charge-separating dissociation (Figure 1) in some dicationic electronic states, conferring kinetic stability upon dications in that state. These states with a barrier to charge-separating dissociation are still usually thermodynamically unstable, as the associated minima lie at energies above the asymptote for charge separation; such states are commonly termed "metastable".[23-26,73] As indicated in Figure 2, the effective height and width of the barrier to charge separating dissociation depends on the vibrational energy content of the dication. Thus different vibrational levels of the metastable dication state will have different lifetimes with respect to charge separating dissociation, as the different vibrational levels can tunnel through the barrier with different efficiencies.[74] In practice, on the timescales probed in modern mass-spectrometric experiments, only for vibrational levels very close to the top of the barrier is tunnelling dissociation a practical relaxation pathway for metastable dication states. As the vibrational energy decreases, the width of the barrier to charge separation increases significantly, and the tunnelling lifetime rapidly becomes longer than that required for mass spectrometric detection (microseconds).[75] In fact, when considering the role of dications in energized media, lower lying vibrational levels of metastable dication states have lifetimes to dissociation many orders of magnitude longer than the time between collisions with other species, and the dications can be treated as effectively "stable" species.[36] Indeed, when trying to rationalize the lifetimes of metastable dications in vibronic states lying significantly below the top of the barrier to charge-separation, dissociation *via* a curve crossing to a neighbouring dissociative state, as illustrated in Figure 2, appears to be the principal unimolecular decay pathway.[76] Experimental measurements of the lifetimes of metastable dication states confirm these conclusions.[75,77]

The form of the dicationic potential energy surfaces, as illustrated in Figure 2, can be rationalized in several ways. Extending the arguments presented above, Sentkowitsch and O'Neil[78] accounted for the form of the metastable potential energy curve of the F_2^{2+} dication in terms of the sum of the potential of the isoelectronic O_2 molecule and a simple Coulomb repulsion potential. Such a decomposition of the dicationic potential into a bonding component and a repulsive electrostatic component ties in with the qualitative description, presented above, of metastable dication states resulting when chemical bonding can overcome the electrostatic repulsion. This model is of distinct value when trying to assess the potential stability and structure of a prospective molecular dication. In this situation, considering the structure and energetics of the isoelectronic neutral species and adding a simple repulsive potential provides an estimate of the likely availability of metastable dication states. This simple representation of dicationic metastable states, as separated positive charges held together by chemical bonding, is not though universally applicable. For example, in some dicationic species which involve atoms with widely differing polarizabilities (e.g. CH_3I^{2+}) and electro-negativities, the positive charges can be found to reside predominantly on one atom in certain electronic states.[79]

Given the shortcomings of the simple picture of metastable dication states presented above, a more comprehensive representation of the bonding interactions is required. To this end, as illustrated in Figure 2, one can consider the potentials that arise when assembling a dication (XY^{2+}) from separated moieties. As discussed above, if we allow the approach of X^+ and Y^+ the diabatic potential arising from this interaction will approximate to a monotonically repulsive surface. However, there is another possible dissociation asymptote for XY^{2+}, dissociation to a daughter dication and a neutral: $X^{2+} + Y$. Allowing X^{2+} to approach Y will result in a potential dominated by polarization-attraction at intermediate interspecies separations. As illustrated in Figure 2, the interaction of the diabatic $X^+ + Y^+$ and $X^{2+} + Y$ potentials can result, in the adiabatic limit, in an avoided crossing giving the expected form of a metastable dication state (Figure 2): a kinetically stable minimum with a barrier to charge separating dissociation. In this avoided crossing model, the dicationic potential minimum is still the

result of the competition of "electrostatic" and "bonding" contributions, but without explicit reference to the bonding of the isoelectronic neutral. Considering the dissociation of XY^{2+} under this avoided crossing model (Figure 2), in a diabatic picture, as X^{2+} and Y separate the dissociating system undergoes an intra-system electron transfer at the top of the barrier to transfer to the $X^+ + Y^+$ potential and accesses the asymptote involving charge-separation.[73] As we will see below, this simple model (Figure 2) involving electron transfer at crossings between diabatic surfaces representing X^{2+}+ Y and $X^+ + Y^+$, as well as helping rationalize the existence of metastable dication states, also allows us to explain the key features of their bimolecular electron transfer reactions.

The above analysis indicates why charge-separating dissociation is the principal unimolecular decay mechanism for small molecular dications. However, perusal of Figure 2 leads to the conclusion that for a dication XY^{2+}, if the second ionization energy of one of the moieties making up the dication ($X^+ \rightarrow X^{2+} + e^-$) is low and the first ionization energy of the other moiety is high ($Y \rightarrow Y^+ + e^-$), then the X^{2+} + Y asymptote can lie below the $X^+ + Y^+$ asymptote. As illustrated in Figure 3, this situation should result in thermodynamically stable dication states. Schwartz and co-workers[26] have developed this model and demonstrated the existence of *stable* states for dications composed of atoms with low second ionization energies (e.g. metals) bonded to electronegative atoms with high first ionization potentials (e.g. halogens). For example, the thermodynamically stable AlF^{2+} and SiF^{2+} ions have been generated by removing an electron from the corresponding monocations.[80]

If the energetics of the dication place the neutral loss asymptote (X^{2+} + Y) at energies just above the charge separation asymptote ($X^+ + Y^+$), then the curve-crossing between these two potentials (Figure 2) will move to large interspecies separations. The coupling between these two potentials, at these large interspecies separations, will be weak and energy deposited in the dication XY^{2+} will then favour neutral loss rather than charge separation. Again, this class of energetics is likely to exist in dications involving species with high first ionization energies, such as halogens. Satisfyingly, fluorinated dications, such as CF_3^{2+} and SF_4^{2+} do display a marked tendency for collision-induced neutral loss (CINL) to form CF_2^{2+} + F or SF_3^{2+} + F in accord with these simple models.[81-83]

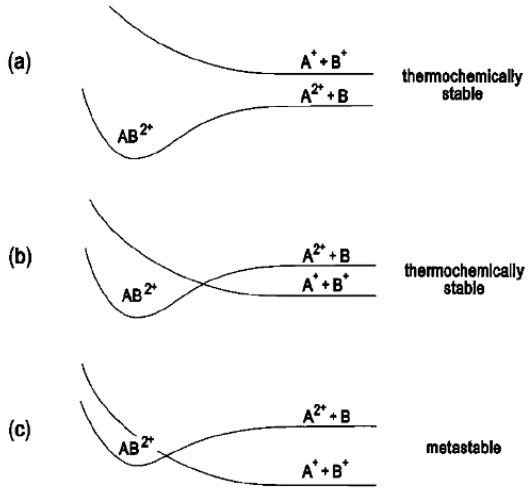

Figure 3 Schematic potential energy curves for an AB^{2+} dication: (a) stable dication with $IE(A^+)<IE(B)$; (b) stable dication with $IE(A^+)>IE(B)$; (c) metastable dication with $IE(A^+)>>IE(B)$. Figure after Schroder and Schwarz.[26]

3. Coincidence techniques

Several classes of experimental techniques have contributed to our current understanding of the formation, structure and unimolecular decay of molecular dications. For example, Auger spectroscopy, laser predissociation spectroscopy and double-charge transfer spectroscopy have provided valuable probes of dicationic vibronic structure.[84-93] However, there is no doubt that the class of experiments that have contributed the most to our understanding of the properties of molecular multiply-charged ions are the wide variety of coincidence experiments that have been employed to probe the formation and dissociation of these species.[37-41] Coincidence experiments, in general, involve the detection of more than one product from a single occurrence of a physical process of interest. Such techniques are used extensively, of course, in particle physics. To illustrate the power of a simple coincidence technique, let us consider the formation of a dication by photoabsorption followed by the dication's unimolecular dissociation *via* the charge-separating pathway discussed above:

$$XY + h\nu \rightarrow XY^{2+} + e_1^- + e_2^- \quad (1)$$

$$XY^{2+} \rightarrow X^+ + Y^+ \quad (2)$$

Simple mass spectrometric probing of this ionization process would detect X^+ and Y^+, but these fragment ions will also be formed, in far greater numbers, by dissociative single ionization which commonly competes with double ionization. To focus successfully on the products of double ionization our experimental technique needs to detect *pairs* of ions and the most straightforward coincidence technique to implement involves recording ion-ion coincidences. To record these coincidence spectra the photon source and gas source are arranged so that the ionization events occur in the source region of a time-of-flight mass spectrometer (TOFMS).[70] Time-of-flight mass spectrometry is ideally suited to this class of coincidence experiments due to the multiplex mass detection capability of the technique; that is, X^+ and Y^+ ions can be detected at the same time, in contrast to a traditional magnetic sector device. The electric field across the source region of the TOFMS is continuously applied, so that when a dissociative double ionization event occurs the X^+ and Y^+ ions are immediately accelerated towards the detector. The detection circuitry is configured so that the first ion arrival (the lighter ion) starts the timing electronics, these days commonly a time-to-digital converter; originally often a time-to-amplitude converter was employed. The timing circuit is stopped by the detection of the second, heavier ion. Thus, the dissociative double ionization event results in the recording of a time-of-flight difference (Δt), which has a characteristic value proportional to the difference between the square roots of the masses of X^+ and Y^+: $\Delta t = k\,[\sqrt{m}(X^+) - \sqrt{m}(Y^+)]$. This measurement of time-of-flight differences is repeated for many events. The histogram of time of flight differences that results will, under the correct conditions, consist of a true coincidence signal (where the X^+ and Y^+ originated from the same dissociation event) at the characteristic time of flight, superimposed upon a background of false coincidences where the X^+ and Y^+ ions detected were formed in different ionization events. Consideration of the rate of true to false coincidences leads to the conclusion that to improve the signal to noise in a coincidence spectrum one must reduce the event rate. A reduced event rate decreases the probability of two different ionization events occurring in the same duty-cycle of the experiment. The form of the coincidence signal in this simple ion-ion coincidence experiment can be readily interpreted to yield the kinetic energy release upon the dissociation of the dication. The value of this kinetic energy release (Figure 2), together with the energy of the dissociation asymptote, can give an indication of the energy of the dication state, a spectroscopy of dications.[94]

These simple ion-ion coincidence experiments proved a powerful probe of the energetics of the unimolecular dissociation reactions of molecular dications. However, over subsequent years the

coincidence experiments employed to study isolated multiply-charged ions became more and more sophisticated detecting various combinations of the charged particles generated in the double ionization process.[37,40,41] For example, coincident detection of the pairs of photoelectrons emitted upon double ionization lead to a photoelectron spectroscopy of dications.[95-97] Indeed, more modern experiments have involved energy-resolved detection of both of the photoelectrons and position-sensitive detection of the two fragment ions allowing an exquisitely detailed probe of the electronic structure and dissociation dynamics of the dication.[98] The increasing sophistication of these multi-parameter coincidence experiments has now been extended to higher levels of ionization providing an elegant and informative probe of the formation and fate of multiply-charged species.[51]

4. Bimolecular reactions of dications

4.1. Electron transfer reactions of atomic dications

An upsurge of interest in the interaction of atomic multiply-charged ions with neutral species (usually atoms) began in the 1970s. Interest in this class of collisions was stimulated, in part, because of their potential relevance in fusion plasmas and other high temperature environments. In these investigations, the focus was often on "fully-stripped" reactant ions (e.g. He^{2+}), although data for partially-stripped dications, such as C^{2+} and N^{2+} was also reported. [99]

The centre-of-mass (CM) collision energies *T* were frequently large, often in the keV range,[100-103] a regime where bond-forming reactivity would not be expected and electron transfer (ET) processes were unsurprisingly the dominant reactive pathway:

$$X^{q+} + Y \rightarrow X^{(q-1)+} + Y^{+} \qquad (3)$$

Indeed, one of the methodologies developed to explain the final state-selectivity in these ET reactions (Landau-Zener theory) has found widespread applicability in accounting for the product yields in the ET reactions of molecular dications at markedly lower collision energies (T < 10 eV).[15,27,28,73,104,105] The primary data provided by these investigations involved the cross sections and final state selectivity of the observed electron transfer process, often as a function of the collision energy. The experimental techniques employed in these investigations usually involved a "crossed beam" approach, where a reactant ion beam, of selected translational energy, interacts with the neutral species. [99] Often translational energy spectroscopy was used to monitor the distribution of electronic states of the products. In this approach, the translational energy changes of the daughter product ion ($X^{(q-1)+}$) which is formed following electron capture from a fast beam of reactant ions (X^{q+}), with a known internal energy distribution, is used to reveal which final ionic states are populated. Photon and electron emission from the nascent product ion states was also sometimes used to reveal the electronic states populated by these ET reactions. [99]

As mentioned above, these high collision energy experiments all adopted a crossed beam methodology. Here, the approach focusses on generating a primary ion beam of known energy and internal state distribution and monitoring the product states following interactions at a known geometry and under single-collision conditions.[15,30] Such experiments are ideal for revealing the detailed state selectivity and dynamics associated with the interaction under study, but the measured energy-resolved cross sections, if they are indeed extracted, have to be integrated over an appropriate energy-distribution function to give cross sections representative of a given temperature.[106] Often, energy resolved cross sections are not available over a wide-enough temperature range for such an integration to be reliable. To overcome this issue, at the expense of some dynamical information, experimentalists turn from "beam" experiments to "swarm" techniques.[107-109] In these swarm

techniques the reactants encounter the neutrals in a multi-collision regime, where the temperature is well defined. This multi-collision characteristic of swarm experiments, often sacrifices the dynamical information that is generated from a beam experiment, but yields reliable data on cross sections at a well-defined temperature. Swarm experiments are often well-suited to probing ion-neutral interactions at lower collision energies.[110] At these energies forming usable ion beams is often highly problematic. The reactivity of multiply charged rare gas dications, at temperatures of 300 K, was probed in a pioneering SIFT experiment.[111] In the SIFT experiment, mass selected ions are injected into an appropriate fast-flowing bath gas (often He) maintained at a given temperature. Collisions with the bath gas thermalize the reactant ions. Further down the flow tube, a neutral reactant is injected into the flow. The attenuation of the reactant ion signal, often monitored using mass spectrometry, as a function of the number density of the neutral reactant can be used to extract rate coefficents for the removal of the reactant ion. The mass spectrometric sampling can also be used to identify the reaction products and associated product branching ratios. Many variations on this basic experimental arrangement have been developed, including, for example, spectroscopic monitoring of the reactants or products. Smith *et al.* showed that at 300 K, single electron transfer reactivity (SET) was the dominant reaction channel and a simple Landau-Zener curve crossing model (described below) accounts for both the reactivity they observed and the changes in that reactivity with the electronic state distribution of the reactants.[111] With a Ne^{2+} reactant, they also observed that double ET forming Ne was competitive with SET when the neutral reactant was Kr or Xe.

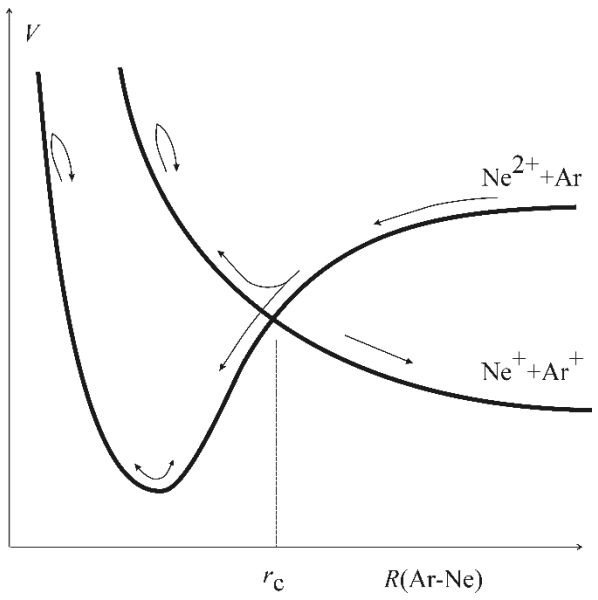

Figure 4 Schematic potential energy curves to illustrate the Landau–Zener model of electron transfer between Ne^{2+} and Ar. Electron transfer occurs at the intersection of a reactant (dication + neutral) potential, which is dominated at large interspecies separations by polarization attraction, and a product potential (monocation + monocation) dominated by Coulomb repulsion. The curve crossing radius r_c is indicated. Taken from reference [27].

4.2. Electrostatic models of dicationic electron transfer

As noted above, a major product channel following the interaction of a dication with a neutral species is often single electron transfer (SET); for example:

$$Ne^{2+} + Ar \rightarrow Ne^{+} + Ar^{+} \quad (4)$$

In the low collision energy regime (T<10 eV), where one might expect the dication-neutral interaction to be long-lived enough for bond-forming chemistry to occur, simple electrostatic models have provided a valuable tool for rationalizing the reactivity observed. Let us begin with considering a simple model for SET based on Landau-Zener theory.[29,73,104,112-115]

As illustrated in Figure 4, and discussed above, as a dication approaches a neutral species [Rxn (4)] the long-range potential will be dominated by the electrostatic interaction between the charge of the dication and the dipole that charge induces in the neutral species; this interaction has a dependence on r, the interspecies distance, of r^{-4}. Of course, as the two reactants approach each other closely, repulsive forces will overwhelm this polarization-attraction potential and the overall interaction will become repulsive (Figure 4). The single electron transfer results in a pair of monocations, the interspecies potential of which will be well represented by a simple Coulombic repulsion. The separation of the reactant and product asymptotes, the energy change of the SET reaction ΔE, corresponds to the difference between the first ionization energy of the neutral collision partner, e.g. $IE(Ar \rightarrow Ar^{+})$ and the second ionization energy of the species that is the dication e.g. $IE(Ne^{+} \rightarrow Ne^{2+})$ (Figure 4); a value of ΔE<0 indicates the SET process is exoergic:

$$\Delta E = IE(Ar \rightarrow Ar^{+}) - IE(Ne^{+} \rightarrow Ne^{2+}) \quad (5)$$

In the Landau-Zener (LZ) model which has proved so effective at rationalizing the SET reactions of molecular dications at lower collision energies, the transfer of the electron from the neutral to the dication occurs at the intersection of these product and reactant potentials – the curve crossing. In the LZ picture it is the interspecies separation of this curve crossing that determines the facility of a single electron transfer event.[27,29,104,115] If the energetics of the collision system are such that the curve crossing lies at a large interspecies separation, the coupling between the reactant and product potentials will be small; the electron will not be able to tunnel efficiently between the two reactants, and electron transfer will be inefficient. Conversely, if the curve crossing lies a small interspecies separation, the coupling between the reactant and product potentials will be large and electron transfer will be efficient, on a single pass through the crossing. However, as illustrated in Figure 4, for electron transfer to be the overall result of the dication-neutral interaction the collision system has to pass though the curve crossing twice, but only swap potentials once. Thus, if curve crossing is at a small interspecies separation, and the coupling between the potentials is large, then an electron will be transferred as the reactants pass through the curve crossing on their approach but also as the collision system passes through the crossing for the second time, as the species separate; thus, no net electron transfer results. That is, if the probability of remaining on the same potential on one pass though the curve crossing is δ, the probability of overall electron transfer P is given by P = δ(1- δ). Inspection of P, shows that efficient electron transfer requires an intermediate coupling regime where δ is close to 0.5, giving a maximum value of P. So, for net electron transfer to result from a dication–neutral interaction we need the curve crossing to occur at an interspecies separation where the coupling between the reactant and product potentials is neither too weak nor too strong. Analysis of the couplings in this prototypical system shows that if the curve crossing lies between about 2 Å and 6 Å, the coupling is such that efficient electron transfer results.[27,29,104,115] This range of interspecies separations over which electron transfer is efficient is often termed the “reaction window”. As shown in Figure 5, for this simple electrostatic model of the dication-neutral interaction,

the spread of curve crossings which should correspond to efficient electron transfer translates to a reaction window of exothermicities for which electron transfer should be efficient: 2 eV – 6 eV. This application of reaction window theory has allowed the rationalization of the state-selectivity of electron transfer in a variety of dication-neutral collision systems.

4.3. Electron transfer reactions of molecular dications

Following the upsurge of interest in the electron transfer reactions of atomic dications, stimulated by their potential relevance in fusion reactors, an obvious extension was to explore the bimolecular reactivity of molecular dications. Initial investigations of the collisional behaviour of bimolecular dications were made at high (>1 keV) collision energies in conventional mass spectrometers.[100-103,116-124] However, experiments were soon extended to lower collision energies, below 100 eV. At first, the focus of these experiments involved collisions with the rare gases where the major product channels involved electron transfer. For example, initial experiments involved generating beams of metastable CO^{2+}, CO_2^{2+}, OCS^{2+} and CS_2^{2+} ions and detecting the products formed following the interactions with a variety of rare gas atoms.[73,82,104,115,125,126] The surprising observation from these experiments was the dramatic change in the product ion distribution, observed mass spectrometrically, when the neutral collision partner was changed from the light rare gases (He, Ne) to the heavier rare gases (Kr, Xe).

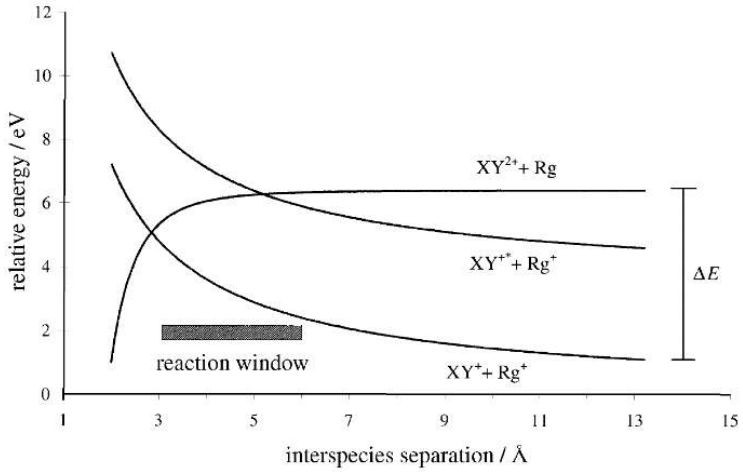

Figure 5 Schematic potential curves to illustrate how, as the magnitude of the reaction exothermicity (ΔE) for an electron-transfer reaction with a neutral rare gas (Rg) atom increases, curve crossings which populate excited states of the molecular monocation (XY^{+}*) may lie in the reaction window whilst population of the ground state of XY^{+} is disfavoured. Taken from reference [73].

The above variation in reactivity was well rationalized by the simple electrostatic model based on reaction window theory described above.[104,115] With He as the collision partner, an atom which has a large first ionization energy, SET was often endoergic; that is [Eq. (5)] the first ionization energy of the rare gas is larger than the second ionization energy of the molecule. Under the reaction window model this means there is no curve crossing between the reactant and product potentials and SET should be disfavoured. This absence of electron transfer in collisions between dications and He was confirmed experimentally with the product ion distribution being dominated by collision-induced dissociation (CID). In the CID process, which has also been extensively observed in collisional experiments involving dications carried out at high collision energies, the translational energy of the

collision promotes the metastable dication to a higher-lying electronic or vibrational state which rapidly undergoes charge separation:

$$CO^{2+} + He \rightarrow [CO^{2+}]^* + He \rightarrow C^+ + O^+ + He \quad (6)$$

Collisions with the heavier rare gases (Ne, Ar) involve neutral species with lower first ionization energies and SET becomes exoergic. These energetics allow curve crossings populating the lowest energy states of the product monocations (e.g. CO^+ and Ar^+) to move into the reaction window and formation of stable states of the molecular monocation is favoured. With the heaviest rare gases (Kr, Xe), which have markedly lower first ionization energies, curve crossings involving the population of low-lying electronic states of the molecular monocations move to low interspecies separations and are disfavoured. In contrast, curve crossings involving the population of excited states of the molecular monocation (Figure 5) move into the reaction window. Often, these electronically excited states of the molecular monocation are unstable and dissociate:

$$CO^{2+} + Kr \rightarrow CO^+(D) + Kr^+ \rightarrow C^+ + O + Kr^+ \quad (7)$$

Thus, with the heavier rare gases the product ion yields are dominated by dissociative SET forming daughter monocations derived from the molecular monocation. This simple model, based on reaction window theory, has been widely used to rationalize the product ion distributions following low energy collisions of molecular dications with a variety of neutral species.

An interesting conclusion arises from the success of the, admittedly simplistic, reaction window model in rationalizing the SET reactivity of dications at low collisions energies. This conclusion is that, at these relatively low collision energies, the translational energy in the collision system cannot efficiently couple the reactant and product potentials if there is no curve crossing. For example in collisions with He, if the SET process is nominally endoergic, even though the translational energy in the collision system is large enough to make the overall SET process exothermic, no SET occurs since there is no curve crossing; the translational energy cannot efficiently couple into the electronic co-ordinates.

4.4. Double Electron Transfer

As noted above, double electron transfer (DET) is observed in some dication-neutral collision systems. If the neutral collision partner is restricted to the rare gases, DET most frequently occurs with Xe, the rare gas with the lowest double ionization energy:

$$CS_2^{2+} + Xe \rightarrow CS_2 + Xe^{2+} \quad (8)$$

DET reactions of dications initially generate a product dication and a neutral species. These DET reactions are therefore intrinsically different from DET reactions of highly charged ions which generate a pair of cationic species.[15,99,127] Restricting ourselves to dicationic DET studied by common experimental arrangements, where only ions are detected and identified, the structure of the product neutral (or neutrals) formed by the DET process is uncertain. In addition, unless coincident detection of products is implemented (see below), simple mass spectrometric detection of a DET process requires the reaction to form a dicationic product that is sufficiently long-lived to be detected. Partly due to the above two caveats, dicationic DET processes remain rather poorly characterized and, in all likelihood, their ion yields under-estimated. DET reactions of dications will become exoergic in encounters with more complex neutrals, neutrals which have correspondingly lower double ionization energies. The experimental observation that DET channels become active when the process becomes exoergic hints that perhaps a curve crossing model, similar to that devised to rationalize SET, could be used to account for the occurrence of DET. Considering such a simple electrostatic model for DET, the question arises as to whether the pair of electrons are transferred between the neutral and the

dication concertedly, at the intersection of an M^{2+} + X potential and an M + X^{2+} potential, or sequentially.[128] In the sequential mechanism the reactive system moves from the M^{2+} + X potential to the M + X^{2+} potential via an intermediate M^{+} + X^{+} potential. As illustrated in Figure 6, these two models are intrinsically different. In the concerted DET model, both the reactant and product potentials are of the dication+neutral form and thus the curve crossing occurs, under this simple electrostatic model, due to the difference in polarizabilities of the neutral reactant and the neutral product. Under such a model one would conclude that DET should be efficient when the exoergicity of the DET reaction was quite small. Conversely, the sequential DET model should allow access to product asymptotes with a larger exoergicity. Definitive conclusions on the mechanism of the DET process are yet to be drawn. However, it is fair to say that the available data point towards the operation of the concerted process, but more extensive investigation of the available data is required.[128]

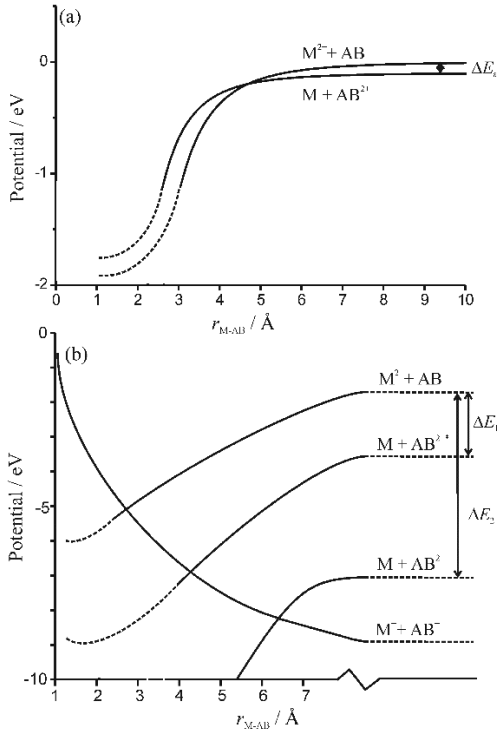

Figure 6 Schematic potential energy curves for (a) concerted and (b) sequential double-electron transfer following the reaction of M^{2+} with AB. In (a) ΔE_a indicates the small reaction energy which is required for the curve crossing to lie in the reaction window for the concerted mechanism. In (b) the sequential mechanism involves an initial single-electron-transfer to the repulsive potential corresponding to a pair of monocations. The system may then remain on this potential, resulting in single electron-transfer, or cross again to reach an $M+AB^{2+}$ asymptote. ΔE_1 and ΔE_2 schematically indicate the limiting reaction exothermicities for which this pair of curve crossings will lie in the reaction window, a markedly larger range of exothermicities than for the concerted mechanism illustrated in (a). Taken from reference [128].

4.5. Bond-forming reactions of molecular dications

As mentioned above, initial investigations of the collisional reactivity of molecular dications were carried out at significant collision energies. Under these conditions, the interaction time between the dication and the neutral will be brief. This short interaction time and the high translational energy of the collision system will mitigate against the formation of new chemical bonds (so called bond-forming reactivity) during the dication-neutral interaction. In light of these observations, it is not surprising that the first reported observation of bond-forming chemistry of a molecular dication came at the low collision energies which operate in swarm experiments.[129] Specifically, Chatterjee and Johnsen reported the formation of NO_2^+ following the interaction of O_2^{2+} with NO in an ion drift tube:

$$O_2^{2+} + NO \rightarrow NO_2^+ + O^+ \quad (9)$$

This observation stimulated the first comprehensive investigation of the collisional reactivity of molecular dications with other molecules at collision energies low enough to allow bond-forming chemistry.[130] This survey revealed that a significant number of dication-neutral collision systems generated "chemical" products and kick-started a period of intensive experimental investigation of these unusual reactive processes. The sections below discuss some of the key findings emerging from this exciting period of experimental work. These examples have been chosen to both illustrate our current understanding of dicationic physical chemistry but also to demonstrate the variety of experimental techniques that have been employed to study these ion-molecule reactions.

4.5.1. The reaction of CF_2^{2+} with H_2.

The initial survey of dicationic reactivity mentioned above [130] used a relatively simple technique involving two successive mass spectrometric stages (MS-MS) to identify and quantify the products of the interactions of molecular dications with neutral molecules. Dications were generated by electron ionization of a precursor molecule (e.g. CF_4) in a low pressure ion source. Careful control of the precursor gas pressure in such dication sources is essential for generating sufficiently intense dication beams. Sufficient gas pressure is, of course, required to provide precursor molecules to be ionized. However, if the precursor gas pressure is too high in the source, dication-neutral reactions rapidly deplete the number of dications that can be extracted to form a dication beam.[131] In the original experiments, dications extracted from the source were mass-selected by a quadrupole mass spectrometer, refocused with a set of ion optics and passed through a collision region where they encountered the neutral reactant under single-collision conditions.[132] After the interactions in the collision region, ions flew on into the source region of a TOFMS. The TOFMS was oriented perpendicularly to the direction of the dication beam and is used to identify and quantify the ionic products. Under single-collision conditions, most of the reactant ions experience no collisions at all, but we are also certain that no products can be formed by the products from an initial collision subsequently interacting with a second neutral molecule. The experimental configuration described above requires the ionic products to have significant laboratory frame velocities in the direction of the dication beam to allow them to exit the collision region and enter the source region of the TOFMS.[104,115] This constraint complicated the interpretation of the ionic intensities from these early experiments, but, despite this geometric drawback, this experimental arrangement proved very effective at identifying new bond-forming reactions of molecular dications. For example, significant yields of a bond-forming product were observed following the collisions of CF_2^{2+} with H_2:

$$CF_2^{2+} + H_2 \rightarrow HCF_2^+ + H^+ \quad (10)$$

The significant product ion yield from this bond-forming reaction made it an ideal candidate for subsequent investigation by a classic experimental arrangement employed to study the dynamics of ion-molecule reactions: an angularly resolved crossed-beam mass spectrometer.[29,30,133] In brief,

this experimental technique, which had been used extensively to investigate the dynamics of monocation-molecule reactions, generates a mass-selected beam of the ion of interest. This ion beam is decelerated and interacts perpendicularly with a chopped jet of the neutral reactant. Ions exiting the interaction region can pass through a stopping potential analyser into a detection mass spectrometer. The stopping potential analyser allows control of the energy of the ions reaching the detection mass spectrometer. The detection mass spectrometer, which only accepts ions from a small range of scattering angles, can be rotated about the interaction reaction allowing the determination of the masses and energies of the product ions as a function of their scattering angle. This dataset allows construction of a scattering diagram for the formation of the relevant products. Such scattering diagrams provide a powerful probe of the dynamics of the ion-molecule reactions of interest. The scattering diagram for the formation of CF_2D^+, *via* the CF_2^{2+} + D_2 analogue of reaction (10), is shown in Figure 7.

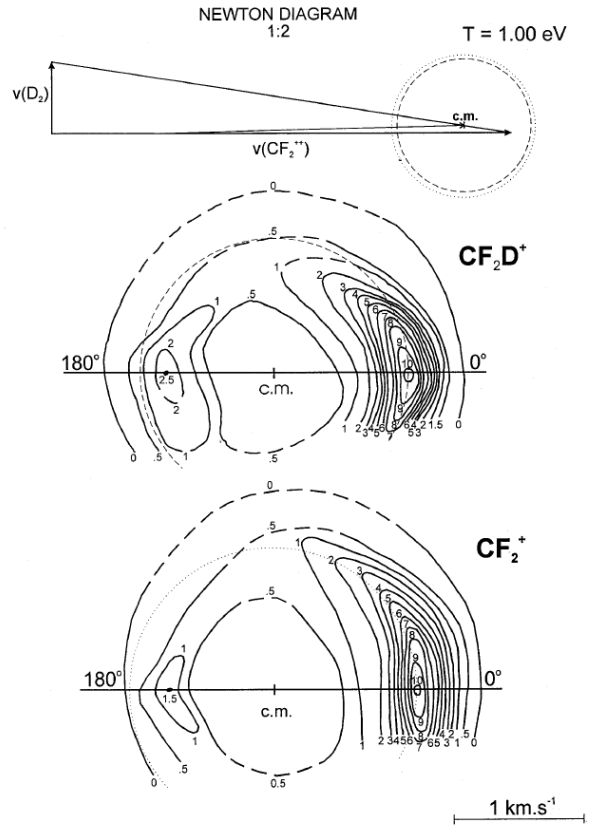

Figure 7 Contour scattering diagrams of the angular and energetic distributions of the products CF_2D^+ and CF_2^+ from bond-forming and SET reactions of CF_2^{2+} with D_2 at a centre-of-mass collision energy of T = 1 eV. The horizontal line shows the direction of the relative velocity vector, c.m. marks the position of the tip of the centre-of-mass velocity vector. The upper panel shows the respective Newton diagram (scale 1:2); the circles in it correspond to the circles drawn through the angular maxima in the scattering diagrams of CF_2D^+ (dashed) and CF_2^+ (dotted). Taken from reference [133].

The scattering diagram in Figure 7 shows clearly that the CF_2D^+ product is strongly forward scattered. That is, the DCF_2^+ product's velocity is strongly orientated in the same direction as that of the reactant CF_2^{2+} dication. This forward scattering clearly indicates the CF_2^{2+} dication flies past the D_2 molecule, stripping a D^- species from the neutral at a significant interspecies separation as it passes. Such dynamics results in the DCF_2^+ product continuing in essentially the same direction as the velocity of the reactant dication. Very similar dynamics, with strong forward scattering, is also observed for dicationic electron transfer reactions.[105,133] This similarity between the formation of HCF_2^+ and the electron transfer dynamics, lead to a picture of the transfer of the hydride ion from H_2 to CF_2^{2+} as a "heavy electron transfer". A similar model of had been previously proposed for formation of MH^+ ions from the reactions of transition metal dications with organic molecules.[134]

Investigations of different collision systems (e.g. CO_2^{2+}+ H_2) involving the formation of new chemical bonds, with this same angular scattering approach, revealed that with molecular hydrogen the forward scattering of the bond forming products was often complemented by another route to the products involving "forward-backward" scattering.[135] As we will see in the section below, such scattering implicated the involvement of a collision complex in the reaction pathway.

4.5.2. The reaction of O_2^{2+} with CH_4.

As described in the section above, the angular scattering of the product ions provides a powerful diagnostic of the mechanism of a dication-molecule reaction. However, "classical" ion-chemistry experiments, although of proven utility for studying the dynamics of monocation reactions, possess some shortcomings when applied to investigate dication chemistry. Firstly, most dication reactions (see below) generate pairs of monocationic products, sometimes accompanied by neutral species. Take for example the reaction:

$$O_2^{2+} + CH_4 \rightarrow HCO^+ + H^+ + [2H + O] \qquad (11)$$

A simple "traditional" ion-molecule technique, using conventional mass spectrometry, might detect the HCO^+ ion. Protons might also be detected, but those protons could also be formed by a dissociative electron transfer reaction where the primary CH_4^+ product of SET then dissociates to give H^+. Thus, a simple, one-dimensional, mass spectrometric technique cannot easily *fully* elucidate the form of the reactivity in dication–neutral reactions. Secondly, in the angularly resolved experiment described above, the mass spectrometer has to be rotated to different positions to gather the angularly resolved dataset. This rotation extends and complicates the data acquisition process. In addition, at some collision energies, there may be some regions of the angular scattering space that are not instrumentally accessible due to physical constraints. These two shortcomings in the application of conventional techniques to study dication-molecule collisions may be overcome by the application of a coincidence methodology to study these processes.

As explained above, a coincidence methodology involves detecting two or more of the species formed in a reactive event, and highly sophisticated coincidence methodologies have been developed to detect the products from dissociative double photoionization of isolated molecules.[37,41] Thus, since many dication-molecule reaction generate pairs of monocations, a logical means to investigate these reactions more thoroughly is to develop an ion-ion coincidence methodology for their study.[28,136] A piece of apparatus implementing such a coincidence methodology is illustrated in Figure 8.

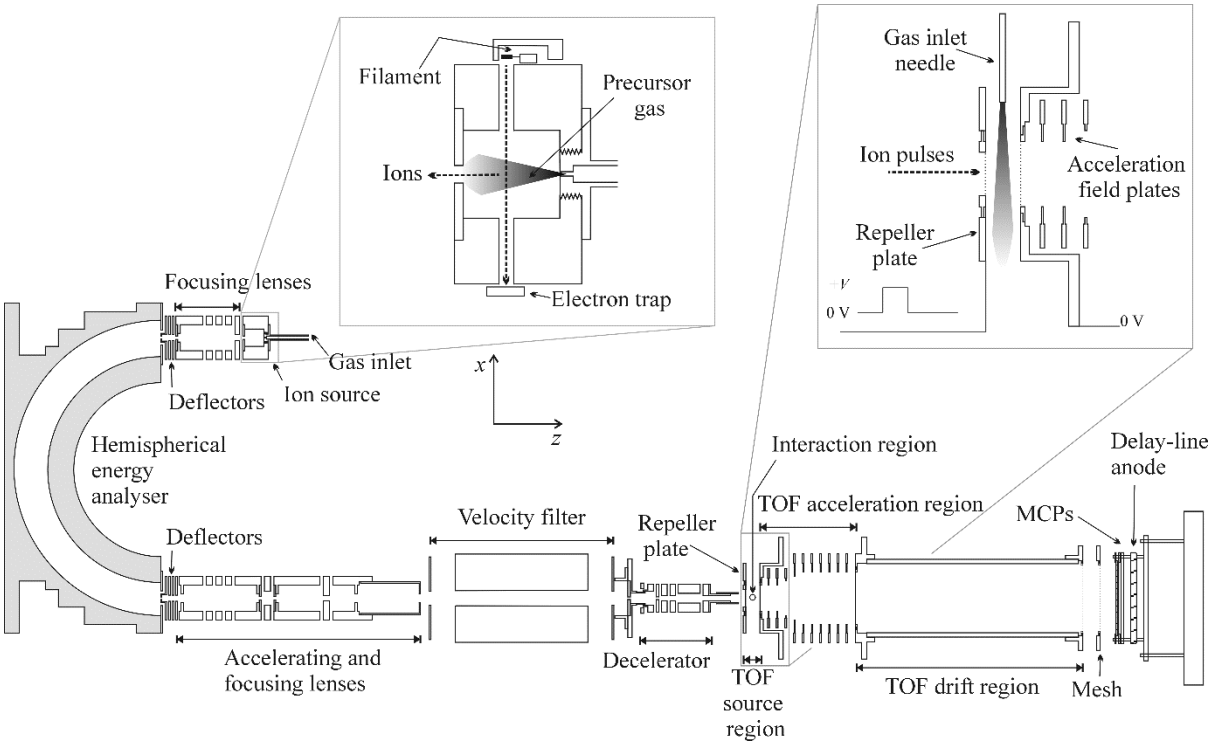

Figure 8 Schematic of the apparatus employed for the PSCO experiments described in this article. Inset in the figure are enlargements of the ion source and the dication–neutral interaction zone. The latter region is situated in the source region of the TOF-MS. Taken from reference [28].

In the apparatus illustrated in Figure 8,[28,136] ions are extracted from a low-pressure ionization source and focussed into a hemispherical energy analyser. The energy-selected ion beam emerging from the analyser is pulsed (1μs pulses at 30 kHz) by sweeping it across an aperture. The ion pulses are then accelerated and focussed into a region of crossed electric and magnetic fields which acts as a velocity filter. Since the ions are selected by their kinetic energy by the hemispherical energy analyser, further selection by velocity leaves just ions of the required mass to charge ratio (e.g. m/z = 22 for CO_2^{2+}) in the ion pulses. These dication pulses then enter an electrostatic decelerator which reduces their kinetic energy to below 8 eV in the laboratory frame. The ion pulses then enter a field-free region where they encounter an effusive jet of the neutral collision partner. This collision region also serves as the source region of a linear TOFMS. Following the interaction of a dication pulse with the neutral gas, an electric field is applied across the collision region to accelerate the ions into a second electric field and then on, via a field-free drift tube, to a position sensitive detector (PSD). The short temporal duration of the ion pulse, and its constrained kinetic energy, means that the dication pulse is well localized in space and, hence, the dication-neutral interactions occur in a restricted time interval before the extraction pulse is applied to the collision region. The TOFMS is also of a second-order focussing design,[137] which maximizes the mass resolution for the non-negligible interaction volume of the ion pulse with the neutral gas. When ions strike the PSD, their time of arrival is recorded as well as their positon in the plane perpendicular to the axis of the TOFMS. The data collection electronics are configured to record events where two ions are detected at the PSD, following one pulse of the repeller plate which extracts the ions from the collision region. Under the correct conditions of low dication flux and a pressure of neutral reactant which corresponds to single-collision conditions, such ion pairs are dominated by the monocation pairs formed in dication-neutral collisions. The data acquisition software stores the timing and positional data for each ion pair detected, for off-

line processing. Due to the low event rate, the experiment gathers data for many hours to accumulate enough pair events to achieve statistical significance.[28]

The off-line processing of the coincidence dataset yields the masses of the ions and their CM velocities for each reactive event detected. The masses of the ion pairs reveal, in one spectrum, all the different reactive channels that generate pairs of monocations in a given collision system, giving a complete picture of the dication's reactivity.[106] Further analysis involves selecting just the events corresponding to one different reaction channel and examining the correlations between the product ions' velocities to reveal the dynamics of the reactive process.[28] As an example of this analysis, and the insight into the reaction mechanisms of dications it provides, let us consider some new results[138] recorded by the above coincidence experiment following the interaction of O_2^{2+} with CH_4.

The ion pairs detected following collisions of O_2^{2+} with CH_4, at a CM collision energy of T = 4.7 eV reveal a rich range of bond-forming chemistry that appears as a series of minor product channels (branching ratio 8 %) competing with single (83 %) and double (9 %) electron transfer. The double electron transfer reactions are identified by the formation of $O^+ + O^+$ ion pairs, with dynamics characteristic of the unimolecular dissociation of a molecular dication, following the collisions. The bond-forming reactions detected are:

$$O_2^{2+} + CH_4 \rightarrow HCO^+ + H^+ + [2H + O] \quad (12)$$

$$O_2^{2+} + CH_4 \rightarrow HCO^+ + H_2^+ + [H + O] \quad (13)$$

$$O_2^{2+} + CH_4 \rightarrow HCO^+ + H_3^+ + O \quad (14)$$

$$O_2^{2+} + CH_4 \rightarrow HO_2^+ + CH_2^+ + H \quad (15)$$

$$O_2^{2+} + CH_4 \rightarrow HO_2^+ + CH^+ + [2H] \quad (16)$$

$$O_2^{2+} + CH_4 \rightarrow CO_2^+ + H^+ + [3H] \quad (17)$$

$$O_2^{2+} + CH_4 \rightarrow CO_2^+ + H_2^+ + [2H] \quad (18)$$

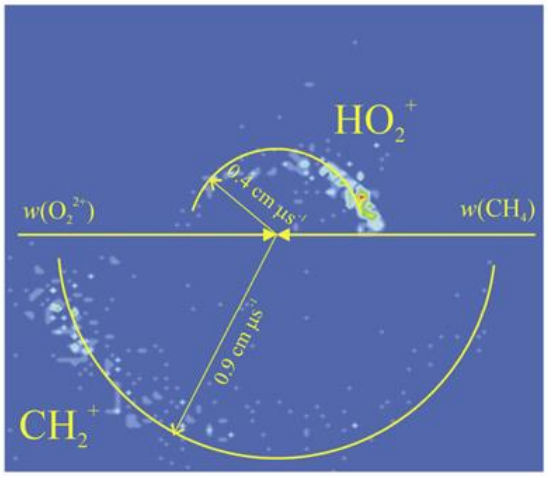

Figure 9 Centre-of-mass frame scattering diagram for the formation of HO_2^+ and CH_2^+ following collisions of O_2^{2+} with CH_4 [Rxn (19)]. The experiments were carried out at a centre-of-mass collision energy of 4 eV. See text for details. The diagram clearly shows the products are strongly forward scattered.

The coincidence technique unambiguously identifies the ion pairs generated in each of these different reactive channels. Accompanying neutral species that are a single atom can also be identified by conservation of mass. However, if more than one atom is involved in the accompanying neutral species the precise connectivity of the neutral(s) cannot be immediately determined. In such cases the neutral species are enclosed in parenthesis in the above chemical reaction equations; although, as we shall see below, very often the precise form of the neutral products can be determined from the reaction mechanism and energetics deduced from the product velocities. A particular power of this coincidence methodology is that for reactions that generate three bodies, for example reaction (15), the CM velocity of the neutral species *w*(H) can be deduced from the measured velocities of the product ions, *w*(HO_2^+) and *w*(CH_2^+), *via* conservation of momentum in the centre of mass frame: [15,28,136]

$$m(HO_2^+)w(HO_2^+) + m(CH_2^+)w(CH_2^+) + m(H)w(H) = 0 \qquad (19)$$

A variety of scattering diagrams are plotted to display and explore the correlations between the velocities of the ionic and neutral products to reveal the reaction mechanism.[15,28,136] Figure 9 shows a centre of mass scattering diagram for the ionic products of reaction (15). In this polar histogram, constructed from the coincidences recorded for a given reactive channel, a point is plotted for each product ion (e.g. H_3^+) detected. For each event, the ion's centre of mass velocity is used as the radial co-ordinate and the scattering angle of the product ion (θ), the angle between the product ion's velocity and the direction of the centre of mass velocity as the angular co-ordinate. Since θ must lie between 0^o and 180^0 data for one ion of the pair can be plotted in the upper semicircle of the diagram, and the data for the other ion in the pair can be plotted in the lower half of the diagram. Note how the complete scattering diagram, for both product ions, is derived from a single experiment.

The scattering in Figure 9 looks very similar to that observed for the formation of DCF_2^+ from collisions of CF_2^{2+} with D_2 (Figure 7), that is the products exhibit strong forward scattering. This form of scattering indicates a direct hydrogen transfer mechanism where the O_2^{2+} flies past the CH_4 and strips a hydride ion from the neutral, leaving the methyl ion in a highly excited state. The HO_2^+ and CH_3^+* ions then separate with the CH_3^+* ions dissociating when significantly distant from the HO_2^+ species. Dissociation of the methyl ion can give CH_2^+ or CH^+, accounting for the similar dynamics observed in the coincidence data for reactions (15) and (16).

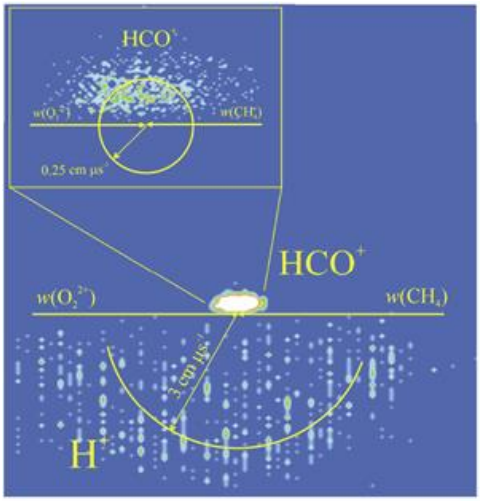

Figure 10 Centre-of-mass frame scattering diagram for the formation of HCO^+ and H^+ following collisions of O_2^{2+} with CH_4 [Rxn(12)]. The experiments were carried out at a centre-of-mass collision energy of 4 eV. See text for details. The diagram clearly shows the products are widely scattered over the full range of available scattering angles.

To learn more about the dynamics of these reactions, we can examine the velocity of the neutral species, a velocity we derive from the product ions' velocities for this three-body process.[15,28,136] Let us consider the dynamics of reactions (12), (13) and (14). These three channels all exhibit a very different form of centre-of-mass scattering, as illustrated in Figure 10, to reactions (15) and (16), discussed in the preceeding pargraph. The scattering diagram in Figure 10 shows the product ions are scattered effectively uniformly over the full range of available scattering angles. This form of scattering is diagnostic of the involvement of a "collision complex" in the reaction pathway. The collision complex, formed by the temporary association of the reactants $[O_2\text{-}CH_4]^{2+}$, has a lifetime significantly longer than its rotational period, before it goes on to break up and form the product ions. The rotation of the collision complex removes any correlation between the relative velocities of the reactants and products. Thus, the product ions are scattered over the full range of scattering angles; in fact one would expect the scattering of the product ions to be isotropic in the centre of mass frame, leading to the sin(θ) style distributions we observe, when plotting data integrated over the azimuthal angle as in Figure 10. To learn more about the mechanism of these reactions, we can further investigate the three-body process (reaction (14)) which forms $HCO^+ + H_3^+ + O$. For each event we detect in this reaction channel, we can determine the velocity of the neutral O atom from the measured velocities of the ionic products. These velocities can then be represented in an internal frame scattering diagram (Figure 11).

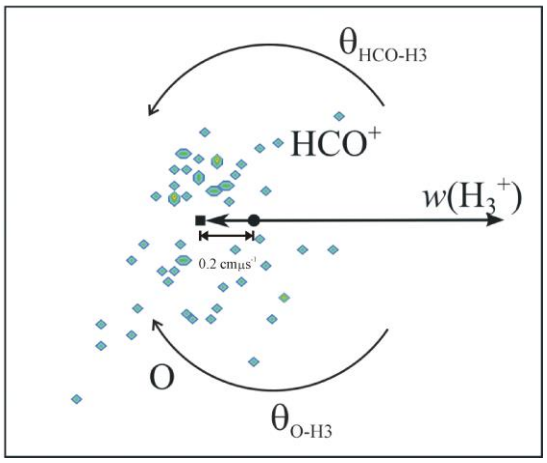

Figure 11 Internal frame scattering diagram for the formation of $HCO^+ + H_3^+ + O$ following collisions of O_2^{2+} with CH_4 [Rxn(14)]. The experiments were carried out at a centre-of-mass collision energy of 4 eV. The diagram shows the relative motions of the three product species. Despite the low counts we can see the HCO^+ and O are scattered in the opposite direction to the H_3^+, and are distributed about a point (marked with a square), the precursor ion velocity, consistent with an initial charge separation of a collision complex $[O_2\text{-}CH_4]^{2+}$ into $H_3^+ + HCO_2^+$ and the subsequent fragmentation of the HCO_2^+ precursor ion. See text for details.

In Figure 11 we again plot the COM velocities of two products (HCO^+ and O) as their radial co-ordinate in the upper and lower halves of the diagram, but the angular co-ordinate is now the angle between these velocities and the third (reference) product, H_3^+ in this case. Although the counts are low, Figure 11 clearly shows that the HCO^+ and O are scattered in the opposite direction to the H_3^+ ion. In addition, again as indicated in Figure 11, the HCO^+ and O velocities are distributed about a point displaced away from the centre of mass. A reaction mechanism consistent with these observations is:

$$O_2^{2+} + CH_4 \rightarrow [O_2\text{-}CH_4]^{2+} \quad (20)$$

$$[O_2\text{-}CH_4]^{2+} \rightarrow HCO_2^{+*} + H_3^+ \quad (21)$$

$$HCO_2^{+*} \rightarrow HCO^+ + O \qquad (22)$$

Here the $[O_2\text{-}CH_4]^{2+}$ lives for long enough, compared with its rotational period, to result in the isotropic scattering of the $HCO_2^{+*} + H_3^+$ products of its decay. When well separated from the H_3^+, the HCO_2^+ ion dissociates to form HCO^+ and O^+. In this situation, conservation of momentum in the dissociation would constrain the momentum of the HCO_2^+ ion to be equal and opposite to the momentum of the H_3^+ ion.[139,140] From the coincidence data, we can determine that the average velocity of the H_3^+ ion is 2.3 cmμs^{-1}, which would constrain the average velocity of the nascent HCO_2^+ ion to 0.2 cm μs^{-1}. This precursor velocity is shown in Figure 11 to be the point about which the HCO^+ and O velocities are distributed, as would be expected if the mechanism detailed in (20)-(22) was operating. If the nascent H_3^+ product is also formed in excited states it may then dissociate to form H^+ or H_2^+. Thus, we can see that reactions (12)-(14) are in fact essentially the same chemical process. The relative intensities of the different channels show that in most reactive encounters the H_3^+ ions dissociate, and thus the counts for channel (14) are low. Although reactions (12) and (13), which are much more intense than reaction (14), are 4-body processes and the neutral velocities cannot be derived unambiguously, the scattering we observe is perfectly consistent with the above model.

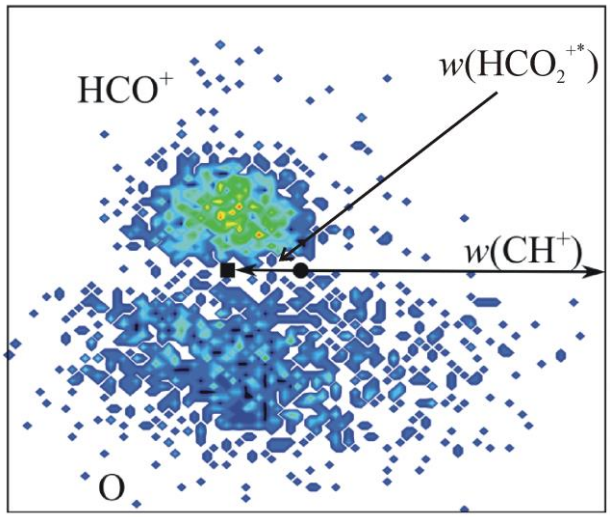

Figure 12 Internal frame scattering diagram for the formation of $HCO^+ + CH^+ + O$ following collisions of O_2^{2+} with C_2H_2 [Rxn(23)]. The experiments were carried out at a centre-of-mass collision energy of 4 eV. The diagram shows the relative motions of the three product species. We can clearly see the HCO^+ and O are scattered in the opposite direction to the CH^+, and are distributed about a point (marked with a square), the precursor ion velocity, consistent with an initial charge separation of a collision complex $[O_2\text{-}C_2H_2]^{2+}$ into $CH^+ + HCO_2^+$ and the subsequent fragmentation of the HCO_2^+ precursor ion. See text for details.

The above general class of mechanism, involving charge-separation of a collision complex to a pair of monocations, followed by dissociation of one or more of the product monocations, appears to be a common reaction motif for molecular dications.[15,28,83,106,128,139-144] For example, Figure 12 shows the internal frame scattering for reaction (23).

$$O_2^{2+} + C_2H_2 \rightarrow HCO^+ + CH^+ + O \qquad (23)$$

Here again, in the internal frame, the velocities of the HCO^+ and O are clearly distributed about a HCO_2^+ precursor velocity derived from the measured velocity of the CH^+ ion.

The above example shows the power of the position-sensitive coincidence technique for probing the dynamics of the reactions of molecular dications. A wide variety of collision systems have been

investigated by this technique and many subtle variations on the two general reaction mechanisms (direct, complexation) illustrated above have been observed.[28] For example, in some collision systems the collision complex clearly loses a neutral species prior to charge separation.[106] However, three specific weaknesses are apparent with the PSCO technique: (1) the coincidence experiment is largely insensitive to dication reactions generating a product dication, rather than a pair of monocations; (2) as with all "beam" experiments, determining absolute cross sections or rates for the different reactive channels is difficult and such rates would be valuable for modelling the role of dications in energized media[31,106] and (3) although the coincidence experiments are carried out at low collision energies, the encounters probed are significantly supra-thermal. These shortcomings are addressed by complementary "swarm" experiments, which are designed to identify and quantify all the ionic products generated by a dication reaction, whilst proving less informative with regard to their detailed dynamics. The information on the dynamics is, of course, available from complementary coincidence experiments. To illustrate this point, the next section discusses a reactive dication-neutral collision system investigated by a swarm experiment.

4.5.3. The reaction of SiF_3^{2+} with N_2

Tandem mass spectrometry involves using mass spectrometry both to select reactant ions and also to identify the charged products formed following the interactions of these reactants with other species. Tandem mass spectrometry, using guided ions beams, has proven a powerful technique for investigating both the charge-separating and charge-conserving chemical reactivity of dications, whist also extending these studies to very low collision energies; collision energies hard to access in crossed-beam experiments.[31,67,110,142,144-153] In a typical experiment, reactant dications are mass selected, often using a quadrupole, from an appropriately designed ion source. The dication beam is then allowed to interact with the neutral reactant at low collision energies in a multipole ion guide which acts as a collision cell.

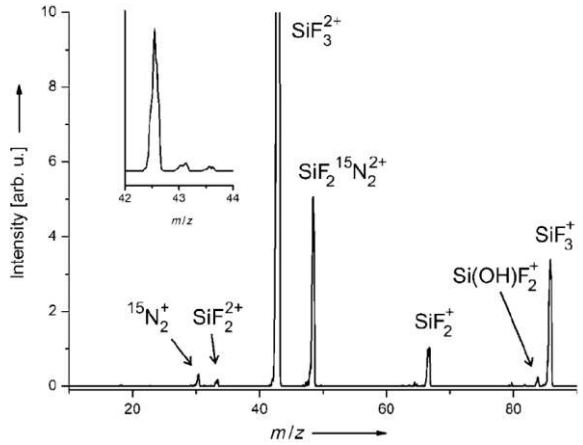

Figure 13 Mass spectrum of products from the reaction of SiF_3^{2+} with $^{15}N_2$ at a nominal collision energy close to 0 eV. The spectrum is normalized to the intensity of SiF_3^{2+} (100). The inset shows a neutral-gain spectrum with Δm = +5.5 (the m/z difference between SiF_3^{2+} and $SiF_2{}^{15}N_2{}^{2+}$), which demonstrates the identity of the silicon containing product ion $SiF_2{}^{15}N_2{}^{2+}$. Taken from reference [150].

The ion guide means that, in principle, all the charged products of the reaction are collected and passed to a second quadrupole for mass analysis. This experimental configuration, with known densities of the collision partner, allows access to rate coefficients for the reactions of the dications. In addition, at the expense of considerable experimental complexity and difficulty, using synchrotron

radiation as the ionizing agent allows dications with constrained and variable internal energies to be created and differences in their reactivity monitored.[145,147]

In a representative experiment, SiF_3^{2+} ions were generated by electron ionization of SiF_4 and allowed to interact with N_2 at collision energies down to thermal velocities.[149] Products due to collision-induced neutral loss and SET were observed but also a significant signal due to the $SiF_2N_2^{2+}$ ion (Figure 13). The yield of this dicationic product peaks at the lowest collision energies. Above the lowest collision energies, the favouring of the bond-forming process over the SET process is perhaps surprising. However, detailed quantum chemical calculations indicate that the reactivity is well-rationalized by initial formation of a $[SiF_3\text{-}N_2]^{2+}$ collision complex which then preferentially loses a neutral F atom to yield the observed $SiF_2N_2^{2+}$ product.[149] Access to the SET asymptotes from the collision complex clearly requires some activation, which explains the increase in the SET yields at the expense of the $SiF_2N_2^{2+}$ yield as the collision energy is raised.

This formation of dicationic products via neutral loss from associative collision complexes is observed for a wide variety of molecular dications at these near thermal collision energies. This reactivity is readily displayed with a wide variety of neutral species, including the rare gases.[110,144,145,147,150,153]

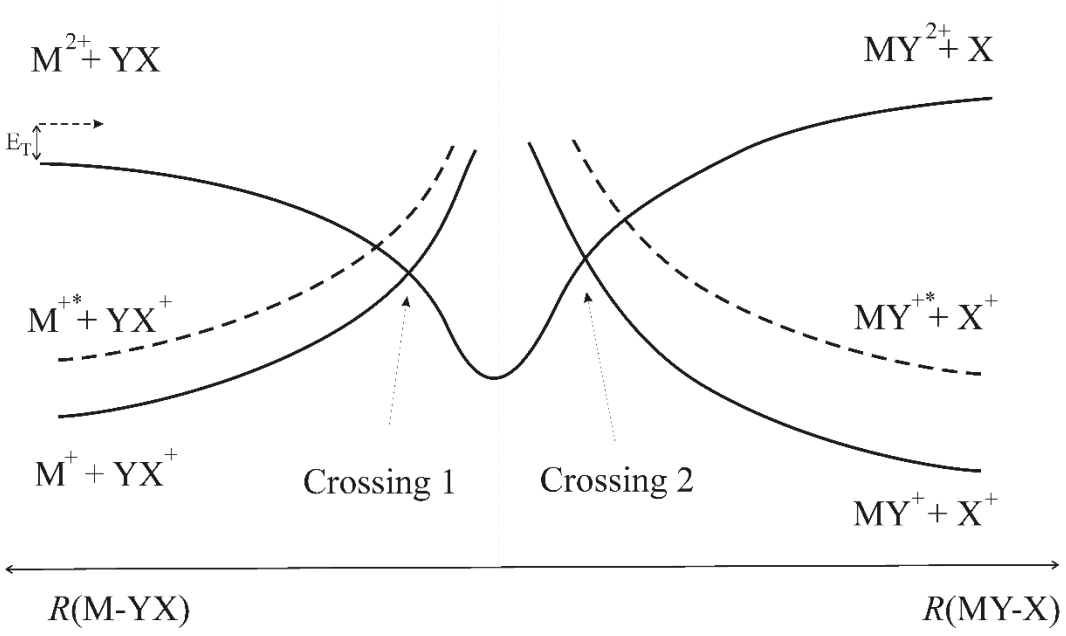

Figure 14 Schematic potential energy surfaces for a bond-forming reaction of a molecular dication, as proposed by Herman.[29] The collision system first encounters a series of curve crossings (crossing 1) in the entrance channel, which potentially lead to SET. If the collision system negotiates these crossings, the dication and neutral can form a collision complex which can then rearrange its bonding and charge-separate to form species with new connectivity. If the separating products undergo electron transfer in the exit channel (crossing 2) a pair of monocations will be formed. Taken from reference [28].

4.5.4. Electrostatic models of dicationic bond-forming reactions

To rationalize this competition between SET, the formation of monocation pairs involving new chemical bonds and the formation of dicationic products, Zdenek Herman developed a simple electrostatic model of the relevant potential energy surfaces which is illustrated in Figure 14.[29,105] The left-hand half of Figure 14 shows the attractive interaction of the dication and neutral (M^{2+} + XY) reactants and the potential crossings which allow simple SET (M^{+} + XY^{+}) as the reactants approach (compare Figure 4). However, Figure 14 illustrates that if the collision system can negotiate its way through these SET crossings, or the complexity of a multi-dimensional collision system means that these crossings are not favoured, then association to form a collision complex $[M\text{-}XY]^{2+}$can occur. This complex can, of course, back dissociate to the reactants or SET products, or separate on a different reactive co-ordinate along a potential leading to dicationic products ($X + MY^{2+}$). This product potential can be crossed by another series of repulsive potentials leading to monocationic bond-forming products (X^{+} + MY^{+}). If one or more of these exit channel curve crossings are in the reaction window, monocationic ions pairs will dominate over dicationic products in the bond-forming channels. Hence, the details of the crossings (or lack of them) between this set of product potentials, and the relative energetics of the monocationic and dicationic bond-forming product asymptotes, will determine whether dicationic or monocationic bond–forming products dominate. The general form of this simple but powerful electrostatic model has been supported by more detailed quantum chemical calculations.[106,135,147,154]

4.5.5. Bond-forming reactions of atomic dications

The form of the generalized potential energy surfaces outlined above are, of course, not specific to molecular dications, just to a reaction between a neutral and a di-positively charged species. Thus, one would expect similar reactivity to be observed for atomic dications as for molecular dications. This is indeed the case, with the experimental techniques outlined above detecting bond- forming reactivity for dications such as Ar^{2+} and I^{2+}, generating both monocationic ion pairs and product dications.[31,155-158] For example, I^{2+} has been shown to react with CS_2 to form both IC^{+} and IS^{+} at collision energies of the order of 6 eV[159] and, at lower collision energies, Ar^{2+} has been shown to react with CO_2 to form ArC^{2+}.[9] Indeed, the reactions of the rare gas dications with molecules at low collision energies, reactions which frequently form dicationic products, have been incorporated into an ever expanding list of methodologies for forming chemical bonds with these noble gas species.

5. Bond-forming reactions of trications

An obvious question arising from the above work is “Is there a bond-forming chemistry of trications”? Experimentally, long-lived atomic trications can be generated from the rare gases, or by dissociative triple ionization of small molecules. Long-lived triply charged ions, derived from organic molecules, are also known mass spectrometrically.[160-164] However, small triply charged molecular ions with lifetimes compatible with collisional experiments are rarer: CS_2^{3+} being a rather isolated example.[165] However, given the success of the above studies of the chemical reactivity of dications, recent experiments have begun to investigate the bond-forming reactivity of small trications. Here we distinguish small molecular trications containing at most a handful of atoms, from triply charged ions of much larger species, such as bio-molecules.[42,166-168] As noted above, in such large molecules, the multiple charges can be well-separated spatially, dramatically reducing the destabilizing effect of the Coulomb repulsion and changing the bimolecular chemistry observed.

Initial experiments to study the chemistry of small trications employed a simple MS-MS technique to probe the products of the interactions of atomic trications (I^{3+} and Xe^{3+}) with a range of neutral molecules.[127] Unsurprisingly perhaps, SET and DET were found to dominate the product ion yields in these collision systems. However, accompanying these electron transfer reactions were minor but

significant yields of unusual ions involving the formation of new chemical bonds. For example, IO^+, IO^{2+}, IS^+ and IS^{2+} are detected following I^{3+} collisions with SO_2 at T = 2 eV (Figure 15); these product ions have a combined yield of about 6% that of I^+. In a different collision system, production of XeF^{2+} and XeF^+ is observed following collisions of Xe^{3+} with CF_4.

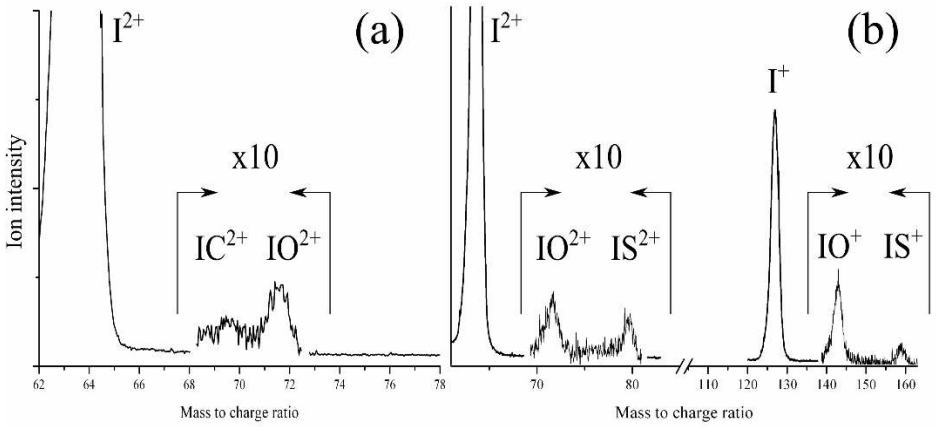

Figure 15 Sections of representative mass spectra recorded following collisions of I^{3+} with (a) CO at a centre-of-mass collision energy of 4 eV and (b) and SO_2 at E = 2 eV. Taken from reference.[127]

The competition between the formation of product dications and monocations in these bond-forming processes has been rationalized by adapting the electrostatic model of dicationic bond-forming reactivity (Figure 14) for tricationic reactants as shown in Figure 16.

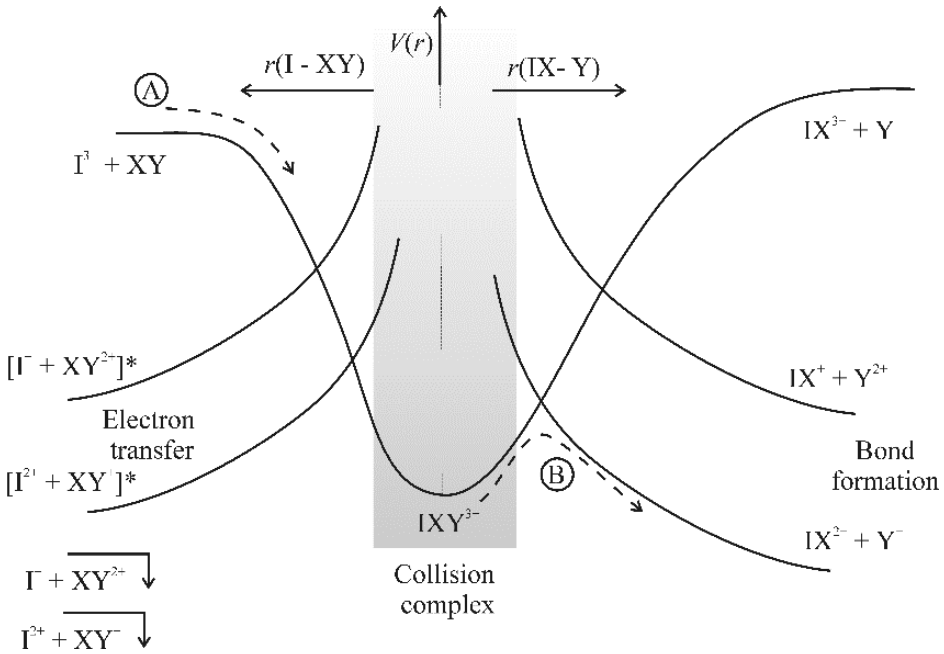

Figure 16 Schematic potential energy surfaces for bond-forming reactivity in trication-neutral collisions. As discussed in the text, the significant exothermicity for the single and double electron transfer processes means that the favoured channels for these reactions are likely to populate excited states of the products, as indicated on the left-hand side of the figure. See text for further details. Taken from reference [127].

In the model displayed in Figure 16,[127] the atomic trication and neutral approach each other along a potential dominated at long-range by polarization attraction. In this entrance channel the reactive system has to negotiate a number of curve crossings which lead to SET or DET. Given that the relative energetics of the electron transfer product asymptotes are likely to be strongly exoergic, the collision system is highly likely to undergo SET or DET. Such a conclusion agrees with the dominance of these processes in the ion yields, but some trication-neutral encounters manage to end up forming collision complexes which can separate in a bond-forming co-ordinate (Figure 16). For bond-forming reactions with diatomic neutrals, the product energetics dictate that the production of a molecular dication together with an atomic monocation is likely to be significantly more exothermic than formation of a molecular monocation and an atomic dication. The more exothermic product channel will be the first curve crossing encountered by the collision system as it separates in the bond-forming co-ordinate. Thus, we would expect atomic dications to react with *diatomic* neutrals to form molecular dications with new chemical bonds, as indeed we observe. [127] However, these energetic constraints are relaxed if the reaction is between a *polyatomic* molecule and an atomic dication and monocations and dications with new chemical bonds should result, again exactly as we observe. The above experiments have principally, for signal strength reasons, been restricted to reactions of atomic trications. However, the formation of a bond-forming product (SF^+) is also observed in challenging experiments involving the generation of a CS_2^{3+} beam and its reaction with CF_3I.[127]

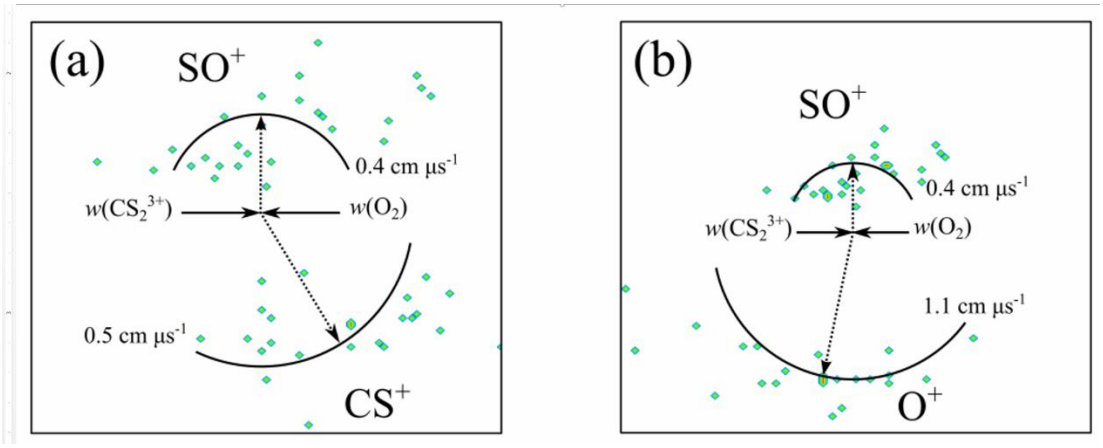

Figure 17 The centre-of-mass scattering diagram, recorded at T = 1.2 eV, for the reaction $CS_2^{3+} + O_2 \rightarrow SO^+ + CS^+ + O^+$. The scattering vectors for (a) $SO^+ + CS^+$ and (b) $SO^+ + O^+$ are given relative to the direction of the velocity of the incident trication.[138]

The above simple analysis indicates that the bond-forming products of trication reactions should involve the formation of collision complexes. To probe the dynamics of these processes we have recently extended our coincidence experiments at UCL to involve the detection of three positively charged ions following the interaction of a trication and a neutral species. In an extension to the analysis of the coincidence data following dication-neutral reactions, detection of three product ions allows us to directly determine the COM velocities for all of the products from a three-body reaction of a trication:

$$CS_2^{3+} + O_2 \rightarrow SO^+ + CS^+ + O^+ \qquad (24)$$

The scattering diagrams for the products of reaction (24) reveal that they are widely scattered in the COM frame, indicative of a collision complex being formed, but highly correlated with each other (Figure 17). This high degree of correlation in the internal frame is what might be expected for a

"Coulomb explosion" of a long-lived triply charged complex, in agreement with the mechanistic conclusions of the simple electrostatic model described above (Figure 16). The weak trication beams make these experiments, and their interpretation, challenging. Much more work remains to be done.

6. Molecular dications in ionospheres and the interstellar medium

There have been recent reviews of the importance and potential role of dications in the chemistry of planetary ionospheres and the chemistry of the interstellar medium. [32,169] With regard to planetary ionospheres, *atomic* dications (O^{2+}, S^{2+}) have been detected in the ionospheres of Earth, Venus and Io.[170-173] Mass spectral peaks which could be a signature of O^{2+} have also been detected in the exosphere of Mars[174] and C^{2+}, Cl^{2+} and S^{2+} have been detected spectroscopically in the Io plasma torus.[175] However, no *molecular* dications have yet been detected in such environments. The problems in identifying molecular dications in planetary ionospheres stem from the difficulties in unambiguous mass spectrometric detection of the expected dications, given the resolution of the remote instrumentation. For example, mass spectrometric signals of N_2^{2+} coincide, and are masked by, those of N^+. Despite this lack of detection, modelling has indicated that molecular dications should be important trace species in the ionospheres of Earth, Mars, Titan and Venus.[33,34,176,177] This modelling indicates that molecular dications have abundances comparable with those of chemically significant monocations in these ionospheres. Recent publications have begun to present data which allow the formation and loss processes which govern the abundances of molecular dications in planetary atmospheres to be correctly included in numerical models of ionospheric chemistry; of course, the loss processes include the reactive channels discussed in this account. Perhaps the most complete dataset encompassing dicationic reactivity is available for the ionospherically relevant processes associated with N^{2+} and N_2^{2+}.[31] Clearly, continued experimental work is required to extend the database of dicationic reactions for which kinetic data are available. Of course, such an experimental effort would be stimulated by the definitive detection of a molecular dication in an ionospheric environment. Thissen *et al.* indicate that such detections are perhaps most likely to arise terrestrially *via* a new generation of mass spectrometric probes,[32] although these authors also advocate the re-inspection of existing datasets, particularly those taken under periods of high solar activity, for undetected emissions, such as those of O^{2+} in the Martian atmosphere. Thissen *et al.* also remark that improved and detailed spectroscopic information on fluorescent transitions of dications such as CO^{2+} and O_2^{2+} may also facilitate their optical detection terrestrially and extra-terrestrially.[32] More recently, interest has focussed on the role of dicationic dissociation in atmospheric escape. Specifically, the fragment ions generated by the charge-separating dissociation of molecular dications formed in in planetary atmospheres possess considerable kinetic energy. This kinetic energy can be enough to allow the fragments to escape into space, contributing to the erosion of the atmosphere. Such considerations appear particularly important for Mars and Titan.[178-181] Clearly, this applied field is in its infancy. However, as general awareness of the potential importance of molecular dications spreads, further examples of their potential involvement in ionospheric science will appear. For example, recent work has indicated the chemistry of MgO^{2+} may affect the measured Mg^+/Mg abundance ratio in the terrestrial ionosphere.[182]

With regard to the role of dications in the interstellar medium (ISM), as discussed by Bohme,[169] multiply-charged *atomic* dications were postulated as important in the astrophysical plasma over 50 years ago.[183,184] Interstellar *molecular* dications, were invoked in the 1980s as a possible contributor to the diffuse interstellar bands and, as a consequence, mechanisms for the formation of multiply charged hydrocarbon molecules in the ISM were considered.[185,186] Interest has also focussed on the role of dicationic states of polycyclic aromatic hydrocarbons (PAHs) in the destruction of these species in interstellar space.[187] More recently, attention has focussed on the potential role

and chemistry of multiply-charged fullerene ions in the ISM. [169] Part of this interest was stimulated by the fact that He^+ is found to efficiently doubly-ionize C_{60} *via* coupled electron-transfer and electron detachment,[188] a similar double ionization pathway to that proposed for PAHs. Some simple chemical models have been developed to illustrate the potential importance of multiply-charged fullerenes in the chemistry of interstellar clouds and circumstellar shells.[189,190] Indeed, Petrie and Bohme developed a "road-map" of the interstellar chemistry associated with C_{60}^{2+} and C_{60}^{3+}, partly to highlight the additional information required to make any such model quantitative.[189] This roadmap builds on extensive laboratory investigations of the chemistry of the multiply-charged ions of fullerenes.[191] This reaction scheme highlights that both the neutralization of dications by electron-capture, and the stability of dications towards radiative dissociation, are poorly characterized at present. As with ionospheric chemistry, the importance of the energetic product ions from dicationic charge separation (so-called "molecular canons") in providing supra-thermal ions in the ISM, ions which can stimulate nominally endothermic chemistry, has also been considered.[169] Intriguingly, experimental investigations have suggested that the bond-forming chemistry of the dications of larger hydrocarbons may provide an efficient route for forming larger organic molecules in the ISM.[192] Specifically, the coupling of medium sized hydrocarbon dications (e.g. $C_7H_6^{2+}$) with 6-14 carbon atoms, with small organic molecules efficiently generates larger dications. This maintenance of the dipositive charge in the reaction products opens the possibility for further coupling cycles, providing a route to significantly larger molecules in the gas-phase. This class of dicationic reactions is particularly valuable, as similar coupling reactions, to form longer carbon chains, *via* the chemistry of hydrocarbon monocations appears inefficient. Indeed, with reference to the preceding paragraph, this coupling chemistry of hydrocarbon dications has also been proposed as being important in the ionosphere of Titan.[193] In summary, as with our understanding of the chemistry of molecular dications in planetary ionospheres, much of the groundwork for detailed modelling of the role of dications in the ISM is already available. What is required, in the opinion of this author, is a definitive detection of a molecular dication in the ISM to kick-start more focused investigations. It was analogous observations of molecular monocations in energized environments that stimulated the explosion of interest in monocationic chemistry, as discussed in the introduction of this article. Further development of our understanding of the role of molecular doubly-charged cations in planetary ionospheres and the ISM now awaits definitive observational evidence; we need to know that dications are "out there".

7. Outlook and Conclusions

Ion-molecule chemistry in the gas-phase has been investigated experimentally for more than 60 years.[194] However, the motivations for these studies, fundamental interest and the applicability of their results to the chemistry of energized media, still remain. The advances in experimental technology that have allowed the investigations of dicationic gas-phase chemistry described above continue, and will undoubtedly allow further progress in the field. One fruitful area for investigation would be making these studies more state-selective. There have been pioneering experiments involving, for example, the generation of dications with energy selected synchrotron radiation, where the reactivity of individual electronic states of dications have been revealed; however, such studies are rare. Indeed, one should expect the development of dicationic chemistry to follow that of monocationic chemistry, where state-selective experiments followed the initial observations of monocation-neutral reactivity. A further avenue for investigation would be to study the interactions between dications and small anions, *via* a merged beam methodology. The advantage of using a dication as the reactant in these studies (rather than a monocation) would be that one of the products will be charged and hence susceptible to efficient mass spectrometric detection. The cross sections

for such reactions should be large, and simple association reactions could well be possible, generating unusual molecules and interesting bonding patterns.

In comparison to 25 years ago, we now have a good picture of the chemistry that occurs in the interactions of small dications and trications with neutral molecules. Electron transfer, which is well modelled by Landau-Zener theory is very often the dominant reactive channel. However, in most collision systems the reactants can associate more closely and access product channels involving the formation of new chemical bonds. Simple electrostatic models provide a rationalization of the reactivity that is observed and provide a good level of predictive power for the chemistry that results.

8. Acknowledgements

SDP acknowledges the help and inspiration of many co-workers both at UCL and further afield. In London, the experimental results presented would not have been obtained without the work of MAP, JDF, FEG, Jess Lockyear, Claire Rickets, Sarah Harper, Paul Burnside and Sunny Hu. The support of Nik Kaltsoyannis whilst the authors dabbled with computational chemistry is also appreciated.

It is important, given the looming Brexit, to recognize the progress in our understanding of dicationic reactivity which took place as a consequence of MCInet - an EU Framework 4 programme. This network established a long-lasting web of, often on-going, collaborations. This EU support fostered interactions between SDP and Zdenek Herman, Detlef Schröder, Jana Roithová, Odile Dutuit, Roland Thissen, Davide Bassi, Paolo Tosi, Daniela Ascenzi, Christian Alcaraz, and many others. The ideas generated by these interactions are much appreciated. Of course, the financial assistance of the EU for this network and the EPSRC and UCL for further financial support is gratefully acknowledged.

9. References

[1] D. Smith *Chem. Rev.* **92** (1992) 1473

[2] D. Smith and N.G. Adams *J. Chem. Soc. Faraday Trans.* **85** (1989) 1613

[3] D. Smith and P. Spanel *Mass Spec. Rev.* **14** (1995) 255

[4] S. Petrie and D.K. Bohme *Mass Spec. Rev.* **26** (2007) 258

[5] D.K. Bohme and H. Schwarz *Angew.Chem.Int.Ed.* **44** (2005) 2336

[6] A. Bultel and B.G. Cheron (2005) in *DR2004: Sixth International Conference on Dissociative Recombination: Theory, Experiments and Applications (Journal of Physics Conference Series)* Wolf A, Lammich L, Schmelcher P (eds), vol 4, p 205

[7] A.B. Fialkov *Progress in Energy and Combustion Science* **23** (1997) 399

[8] A. Fridman (2008) *Plasma Chemistry*. Cambridge Univ. Press, Cambridge

[9] P. Tosi, D. Ascenzi, P. Franceschi and G. Guella *Plasma Sources Science & Technology* **18** (2009) 034005

[10] T.P. Snow and V.M. Bierbaum (2008) in *Annual Review of Analytical Chemistry* vol 1, p 229

[11] E. Vigren, M. Galand, R.V. Yelle, A. Wellbrock, A.J. Coates, D. Snowden, J. Cui, P. Lavvas, N.J.T. Edberg, O. Shebanits, J.E. Wahlund, V. Vuitton and K. Mandt *Icarus* **248** (2015) 539

[12] P.H. Yih, V. Saxena and A.J. Steckl *Phys. Status Solidi B-Basic Res.* **202** (1997) 605

[13] H. Nilsson, G.S. Wieser, E. Behar, C.S. Wedlund, E. Kallio, H. Gunell, N.J.T. Edberg, A.I. Eriksson, M. Yamauchi, C. Koenders, M. Wieser, R. Lundin, S. Barabash, K. Mandt, J.L. Burch, R. Goldstein, P. Mokashi, C. Carr, E. Cupido, P.T. Fox, K. Szego, Z. Nemeth, A. Fedorovn, J.A. Sauvaud, H. Koskinen, I. Richter, J.P. Lebreton, P. Henri, M. Volwerk, C. Vallat and B. Geiger *Astron. Astrophys.* **583** (2015) 8 A20

[14] J.M. Farrar and W.H. Saunders (1988) *Techniques for the Study of Ion-Molecule Reactions*. Wiley, New York

[15] S.D. Price *Reference Module in Chemistry, Molecular Sciences and Chemical Engineering* (2015) DOI:10.1016/B978-0-12-409547-2.10964-3

[16] N.G. Adams and D. Smith *Int. J. Mass Spectrom. Ion Process.* **21** (1976) 349

[17] M. Baer and C.Y. Ng in *Advances in Chemical Physics* Prigogine I, Rice SA (eds), (2009), vol 82, Wiley, New York

[18] V. Vuitton, O. Dutuit, M.A. Smith and N. Balucani (2014) in *Titan: Interior, Surface, Atmosphere, and Space Environment* Cambridge Univ. Press, Cambridge p 224

[19] J.J. Thompson (1921) *Rays of Positive Electricity*. Longmans, Green and Co., London

[20] R. Conrad *Physik. Z.* **31** (1930) 888

[21] A. Vaughan *Physical Review* **38** (1931) 1687

[22] K.E. McCulloh, T.E. Sharp and H.M. Rosenstock *J.Chem.Phys.* **42** (1965) 3501

[23] M. Larsson *Comm. Atom. Molec. Phys.* **29** (1993) 39

[24] D. Mathur *Phys. Rep.* **225** (1993) 193

[25] D. Mathur *Phys. Rep.* **391** (2004) 1

[26] D. Schroder and H. Schwarz *J. Phys. Chem. A* **103** (1999) 7385

[27] S.D. Price *Phys.Chem.Chem.Phys.* **5** (2003) 1717

[28] S.D. Price *Int. J. Mass Spectrom.* **260** (2007) 1

[29] Z. Herman *Int. Rev. Phys. Chem.* **15** (1996) 299

[30] Z. Herman *Int. J. Mass Spectrom.* **378** (2015) 113

[31] O. Dutuit, N. Carrasco, R. Thissen, V. Vuitton, C. Alcaraz, P. Pernot, N. Balucani, P. Casavecchia, A. Canosa, S. Le Picard, J.-C. Loison, Z. Herman, J. Zabka, D. Ascenzi, P. Tosi, P. Franceschi, S.D. Price and P. Lavvas *Astrophysical Journal Supplement Series* **204:20** (2013) 1

[32] R. Thissen, O. Witasse, O. Dutuit, C.S. Wedlund, G. Gronoff and J. Lilensten *Phys.Chem.Chem.Phys.* **13** (2011) 18264

[33] G. Gronoff, J. Lilensten, C. Simon, O. Witasse, R. Thissen, O. Dutuit and C. Alcaraz *Astron. Astrophys.* **465** (2007) 641
[34] C. Simon, J. Lilensten, O. Dutuit, R. Thissen, O. Witasse, C. Alcaraz and H. Soldi-Lose *Ann. Geophys.* **23** (2005) 781
[35] J. Lilensten, O. Witasse, C. Simon, H. Solidi-Lose, O. Dutuit, R. Thissen and C. Alcaraz *Geophys. Res. Lett.* **32** (2005) L03203
[36] O. Witasse, O. Dutuit, J. Lilensten, R. Thissen, J. Zabka, C. Alcaraz, P.L. Blelly, S.W. Bougher, S. Engel, L.H. Andersen and K. Seiersen *Geophys. Res. Lett.* **29** (2002) 1263
[37] J.H.D. Eland *J. Electron. Spectrosc. Relat. Phenom.* **112** (2000) 1
[38] J.H.D. Eland, P. Linusson, M. Mucke and R. Feifel *Chem.Phys.Lett.* **548** (2012) 90
[39] R. Feifel, J.H.D. Eland, L. Storchi and F. Tarantelli *J.Chem.Phys.* **125** (2006) 194318
[40] F. Penent, P. Lablanquie, R.I. Hall, J. Palaudoux, K. Ito, Y. Hikosaka, T. Aoto and J.H.D. Eland *J. Electron. Spectrosc. Relat. Phenom.* **144** (2005) 7
[41] T. Arion and U. Hergenhahn *J. Electron. Spectrosc. Relat. Phenom.* **200** (2015) 222
[42] T.Y. Huang and S.A. McLuckey (2010) in *Annual Review of Analytical Chemistry, Vol 3 (Annual Review of Analytical Chemistry)* Yeung ES, Zare RN (eds), vol 3, p 365
[43] A. Kramida, Y. Ralchenko and J. Reader NIST Atomic Spectra Database (version 5.4) (2016) http://physics.nist.gov/asd [November 2016] National Institute of Standards and Technology Gaithersburg, MD.
[44] I. Bray, D.V. Fursa, A.S. Kadyrov, A.T. Stelbovics, A.S. Kheifets and A.M. Mukhamedzhanov *Phys. Rep.* **520** (2012) 135
[45] J.H.D. Eland (2009) in *Advances in Chemical Physic (s)* Rice SA (ed) vol 141, p 103
[46] A. Huetz, P. Selles, D. Waymel and J. Mazeau *J. Phys. B.* **24** (1991) 1917
[47] C. Miron and P. Morin *Nucl. Instrum. Meth. A* **601** (2009) 66
[48] I. Nenner, P. Morin, P. Lablanquie, M. Simon, N. Levasseur and P. Millie *J. Electron. Spectrosc. Relat. Phenom.* **52** (1990) 623
[49] M. Simon, P. Morin, P. Lablanquie, M. Lavollee, K. Ueda and N. Kosugi *Chem.Phys.Lett.* **238** (1995) 42
[50] K. Ueda and J.H.D. Eland *J. Phys. B.* **38** (2005) S839
[51] P. Kolorenc, V. Averbukh, R. Feifel and J. Eland *J. Phys. B.* **49** (2016) 082001
[52] J.A. Syage *Phys. Rev. A* **46** (1992) 5666
[53] T.D. Mark (1985) in *Electron Impact Ionization* Mark TD, Dunn GH (eds), Springer-Verlag, New York p 137
[54] M.R. Bruce and R.A. Bonham *J. Mol. Struct.* **352** (1995) 235
[55] E. Mark, T.D. Mark, Y.B. Kim and K. Stephan *J.Chem.Phys.* **75** (1981) 4446
[56] H.C. Straub, B.G. Lindsay, K.A. Smith and R.F. Stebbings *J.Chem.Phys.* **105** (1996) 4015
[57] H.C. Straub, B.G. Lindsay, K.A. Smith and R.F. Stebbings *J.Chem.Phys.* **108** (1998) 109
[58] B.G. Lindsay, M.A. Mangan, H.C. Straub and R.F. Stebbings *J.Chem.Phys.* **112** (2000) 9404
[59] P. Calandra, C.S.S. O'Connor and S.D. Price *J.Chem.Phys.* **112** (2000) 10821
[60] S. Harper, P. Calandra and S.D. Price *Phys.Chem.Chem.Phys.* **3** (2001) 741
[61] S.J. King and S.D. Price *Int. J. Mass Spectrom.* **277** (2008) 84
[62] S.J. King and S.D. Price *J. Chem. Phys.* **134** (2011) 074311
[63] M.D. Ward, S.J. King and S.D. Price *J. Chem. Phys.* **134** (2011) 024308
[64] J.D. Fletcher, M.A. Parkes and S.D. Price *J.Chem.Phys.* **138** (2013) 184309
[65] F. Alcantara, A.H.A. Gomes, W. Wolff, L. Sigaud and A.C.F. Santos *Chem. Phys.* **429** (2014) 1
[66] B.P. Tsai and J.H.D. Eland *Int. J. Mass Spectrom. Ion. Proc.* **36** (1980) 143
[67] P. Franceschi, R. Thissen, O. Dutuit, C. Alcaraz, H. Soldi-Lose, D. Bassi, D. Ascenzi, P. Tosi, J. Zabka, Z. Herman, M. Coreno and M. de Simone *Int. J. Mass Spectrom.* **280** (2009) 119
[68] M. Lundqvist, D. Edvardsson, P. Baltzer, M. Larsson and B. Wannberg *J. Phys. B.* **29** (1996) 499
[69] W. Yu, Z.L. Zhu, C.C. Cheng and D.H. Shi *Can. J. Chem.* **92** (2014) 1041
[70] D.M. Curtis and J.H.D. Eland *Int. J. Mass Spectrom. Ion. Proc.* **63** (1985) 241

[71] J.H.D. Eland *Mol. Phys.* **61** (1987) 725
[72] G. Dujardin, S. Leach, O. Dutuit, P.M. Guyon and M. Richardviard *Chem. Phys.* **88** (1984) 339
[73] S.D. Price *J. Chem. Soc. Faraday Trans.* **93** (1997) 2451
[74] V.V. Nefedova, A.I. Boldyrev and J. Simons *Int. J. Quantum Chem.* **55** (1995) 441
[75] D. Mathur, L.H. Andersen, P. Hvelplund, D. Kella and C.P. Safvan *J. Phys. B.* **28** (1995) 3415
[76] G. Parlant, J. Senekowitsch, S.V. Oneil and D.R. Yarkony *J.Chem.Phys.* **94** (1991) 7208
[77] T.A. Field and J.H.D. Eland *Chem.Phys.Lett.* **211** (1993) 436
[78] J. Senekowitsch and S. Oneil *J.Chem.Phys.* **95** (1991) 1847
[79] J.M. Curtis, A.G. Brenton, J.H. Beynon and R.K. Boyd *Chem. Phys.* **117** (1987) 325
[80] C. Heinemann, D. Schroder and H. Schwarz *J. Phys. Chem.* **99** (1995) 16195
[81] S.D. Price, M. Manning and S.R. Leone *Chem.Phys.Lett.* **214** (1993) 553
[82] Y.Y. Lee, S.R. Leone, P.H. Champkin, N. Kaltsoyannis and S.D. Price *J.Chem.Phys.* **106** (1997) 7981
[83] J.F. Lockyear, M.A. Parkes and S.D. Price *Angew. Chem. Int. Ed.* **50** (2011) 1322
[84] H. Aksela, S. Aksela, M. Hotokka and M. Jantti *Phys. Rev. A* **28** (1983) 287
[85] M. Larsson, P. Baltzer, S. Svensson, B. Wannberg, N. Martensson, A.N. Debrito, N. Correia, M.P. Keane, M. Carlssongothe and L. Karlsson *J. Phys. B.* **23** (1990) 1175
[86] D.M. Szaflarski, A.S. Mullin, K. Yokoyama, M.N.R. Ashfold and W.C. Lineberger *J. Phys. Chem.* **95** (1991) 2122
[87] A.S. Mullin, D.M. Szaflarski, K. Yokoyama, G. Gerber and W.C. Lineberger *J.Chem.Phys.* **96** (1992) 3636
[88] T.E. Masters and P.J. Sarre *J. Chem. Soc. Faraday Trans.* **86** (1990) 2005
[89] R. Abusen, F.R. Bennett, I.R. McNab, D.N. Sharp, R.C. Shiell and C.A. Woodward *J.Chem.Phys.* **108** (1998) 1761
[90] S.G. Cox, A.D.J. Critchley, P.S. Kreynin, I.R. McNab, R.C. Shiell and F.E. Smith *Phys.Chem.Chem.Phys.* **5** (2003) 663
[91] O. Furuhashi, T. Kinugawa, S. Masuda, C. Yamada and S. Ohtani *Chem.Phys.Lett.* **337** (2001) 97
[92] J. Roithova, A. Gray, E. Andris, J. Jasik and D. Gerlich *Acc. Chem. Res.* **49** (2016) 223
[93] J. Jasik, D. Gerlich and J. Roithova *J. Phys. Chem. A* **119** (2015) 2532
[94] J.H.D. Eland, S.D. Price, J.C. Cheney, P. Lablanquie, I. Nenner and P.G. Fournier *Phil. Trans. Roy.Soc. A.* **324** (1988) 247
[95] S.D. Price and J.H.D. Eland *Meas. Sci. Tech.* **3** (1992) 306
[96] J.H.D. Eland *Chem. Phys.* **294** (2003) 171
[97] M. Hochlaf, H. Kjeldsen, F. Penent, R.I. Hall, P. Lablanquie, M. Lavollee and J.H.D. Eland *Can. J. Phys.* **74** (1996) 856
[98] F. Penent, R.I. Hall, R. Panajotovic, J.H.D. Eland, G. Chaplier and P. Lablanquie *Phys. Rev. Lett.* **81** (1998) 3619
[99] R.K. Janev and H. Winter *Phys. Rep.* **117** (1985) 265
[100] J.H. Agee, J.B. Wilcox, L.E. Abbey and T.F. Moran *Chem. Phys.* **61** (1981) 171
[101] D. Mathur, R.G. Kingston, F.M. Harris and J.H. Beynon *J. Phys. B.* **19** (1986) L575
[102] K. Vekey, A.G. Brenton and J.H. Beynon *J. Phys. Chem.* **90** (1986) 3569
[103] Z. Herman, P. Jonathan, A.G. Brenton and J.H. Beynon *Chem.Phys.Lett.* **141** (1987) 433
[104] S.A. Rogers, S.D. Price and S.R. Leone *J.Chem.Phys.* **98** (1993) 280
[105] Z. Herman, J. Zabka, Z. Dolejsek and M. Farnik *Int. J. Mass Spectrom.* **192** (1999) 191
[106] J.F. Lockyear, C.L. Ricketts, M.A. Parkes and S.D. Price *Chemical Science* **2** (2011) 150
[107] P.B. Armentrout *J. Am. Soc. Mass Spectrom.* **13** (2002) 419
[108] P.B. Armentrout *Catalysis Science & Technology* **4** (2014) 2741
[109] E. Teloy and D. Gerlich *Chem. Phys.* **4** (1974) 417
[110] J.F. Lockyear, K. Douglas, S.D. Price, M. Karwowska, K.J. Fijalkowski, W. Grochala, M. Remes, J. Roithova and D. Schroder *J. Phys. Chem. Lett.* **1** (2010) 358
[111] D. Smith, N.G. Adams, E. Alge, H. Villinger and W. Lindinger *J. Phys. B.* **13** (1980) 2787

[112] L. Landau *Phys. Z. Sowjetunion* **2** (1932) 26
[113] E.C.G. Stueckelburg *Helv. Phys. Acta* **5** (1932) 369
[114] C. Zener *Proc. Roy. Soc. Lond. Ser. A* **137** (1932) 696
[115] S.D. Price, S.A. Rogers and S.R. Leone *J.Chem.Phys.* **98** (1993) 9455
[116] G.H. Bearman, F. Ranjbar, H.H. Harris and J.J. Leventhal *Chem.Phys.Lett.* **42** (1976) 335
[117] J.M. Curtis and R.K. Boyd *J.Chem.Phys.* **80** (1984) 1150
[118] M. Hamdan and A.G. Brenton *J. Phys. B.* **22** (1989) L45
[119] V. Krishnamurthi, K. Nagesha, V.R. Marathe and D. Mathur *Phys. Rev. A* **44** (1991) 5460
[120] S.E. Kupriyanov *Soviet Physics-Technical Physics* **9** (1964) 659
[121] W.B. Maier and B. Stewart *J.Chem.Phys.* **68** (1978) 4228
[122] D. Mathur and F.A. Rajgara *Phys. Rev. A* **41** (1990) 4824
[123] C.E. Melton and G.F. Wells *J.Chem.Phys.* **27** (1957) 1132
[124] D.S. Waddell and R.K. Boyd *Int. J. Mass Spectrom. Ion Process.* **93** (1989) 337
[125] J.O.K. Pedersen and P. Hvelplund *J. Phys. B.* **20** (1987) L 317
[126] M. Manning, S.D. Price and S.R. Leone *J.Chem.Phys.* **99** (1993) 8695
[127] J.D. Fletcher, M.A. Parkes and S.D. Price *Chem-Eur.J.* **19** (2013) 10965
[128] M.A. Parkes, J.F. Lockyear and S.D. Price *Int. J. Mass Spectrom.* **280** (2009) 85
[129] B.K. Chatterjee and R. Johnsen *J.Chem.Phys.* **91** (1989) 1378
[130] S.D. Price, M. Manning and S.R. Leone *J. Am. Chem. Soc.* **116** (1994) 8673
[131] S.A. Rogers, P.J. Miller, S.R. Leone and B. Brehm *Chem.Phys.Lett.* **166** (1990) 137
[132] K. Yamasaki and S.R. Leone *J.Chem.Phys.* **90** (1989) 964
[133] Z. Dolejsek, M. Farnik and Z. Herman *Chem.Phys.Lett.* **235** (1995) 99
[134] J.C. Weisshaar *Acc. Chem. Res.* **26** (1993) 213
[135] L. Mrazek, J. Zabka, Z. Dolejsek, J. Hrusak and Z. Herman *J. Phys. Chem. A* **104** (2000) 7294
[136] W.P. Hu, S.M. Harper and S.D. Price *Meas. Sci. Technol.* **13** (2002) 1512
[137] J.H.D. Eland *Meas. Sci. Tech.* **4** (1993) 1522
[138] J.D. Fletcher (2014) Studies of atomic and molecular cations, Ph.D., University College London
[139] J.D. Fletcher, M.A. Parkes and S.D. Price *Int. J. Mass Spectrom.* **377** (2015) 101
[140] M.A. Parkes, J.F. Lockyear and S.D. Price *Int. J. Mass Spectrom.* **365** (2014) 68
[141] M.A. Parkes, J.F. Lockyear and S.D. Price *Int. J. Mass Spectrom.* **354** (2013) 39
[142] F. Feixas, R. Ponec, J. Fiser, J. Roithova, D. Schroder and S.D. Price *J. Phys. Chem. A* **114** (2010) 6681
[143] C.L. Ricketts, D. Schroder, J. Roithova, H. Schwarz, R. Thissen, O. Dutuit, J. Zabka, Z. Herman and S.D. Price *Phys.Chem.Chem.Phys.* **10** (2008) 5135
[144] J. Roithova, C.L. Ricketts, D. Schroder and S.D. Price *Angew. Chem. Int. Edit.* **46** (2007) 9316
[145] C.J. Shaffer, D. Schroder, J. Roithova, E.L. Zins, C. Alcaraz, J. Zabka, M. Polasek and D. Ascenzi *Int. J. Mass Spectrom.* **336** (2013) 17
[146] C.J. Shaffer, D. Schroder, C. Alcaraz, J. Zabka and E.L. Zins *ChemPhysChem* **13** (2012) 2688
[147] E.L. Zins, P. Milko, D. Schroder, J. Aysina, D. Ascenzi, J. Zabka, C. Alcaraz, S.D. Price and J. Roithova *Chem-Eur.J.* **17** (2011) 4012
[148] J. Zabka, C.L. Ricketts, D. Schroder, J. Roithova, H. Schwarz, R. Thissen, O. Dutuit, S.D. Price and Z. Herman *J. Phys. Chem. A* **114** (2010) 6463
[149] J. Roithova, H. Schwarz and D. Schroder *Chem-Eur.J.* **15** (2009) 9995
[150] J. Roithova and D. Schroder *Angew. Chem. Int. Edit.* **48** (2009) 8788
[151] A. Revesz, B. Sztaray, D. Schroder, K. Franzreb, J. Fiser, S.D. Price and J. Roithova *Phys.Chem.Chem.Phys.* **11** (2009) 6192
[152] D. Ascenzi, J. Roithova, D. Schroder, E.L. Zins and C. Alcaraz *J. Phys. Chem. A* **113** (2009) 11204
[153] D. Ascenzi, P. Tosi, J. Roithová, C.L. Ricketts, D. Schröder, J.F. Lockyear, M.A. Parkes and S.D. Price *Phys. Chem. Chem. Phys* **10** (2008) 7121
[154] C.L. Ricketts, S.M. Harper, S.W.P. Hu and S.D. Price *J.Chem.Phys.* **123** (2005) 134322

[155] D. Ascenzi, P. Franceschi, P. Tosi, D. Bassi, M. Kaczorowska and J.N. Harvey *J.Chem.Phys.* **118** (2003) 2159
[156] P. Tosi, W.Y. Lu, R. Correale and D. Bassi *Chem.Phys.Lett.* **310** (1999) 180
[157] P. Tosi, R. Correale, W.Y. Lu and D. Bassi *J.Chem.Phys.* **110** (1999) 4276
[158] P. Tosi, R. Correale, W.L. Lu, S. Falcinelli and D. Bassi *Phys. Rev. Lett.* **82** (1999) 450
[159] J.D. Fletcher, M.A. Parkes and S.D. Price *Mol. Phys.* **113** (2015) 2125
[160] L. Morvay and I. Cornides *Int. J. Mass Spectrom. Ion Process.* **62** (1984) 263
[161] R.J. Vanbrunt and M.E. Wacks *J.Chem.Phys.* **41** (1964) 3195
[162] A.S. Newton *J.Chem.Phys.* **40** (1964) 607
[163] S. Meyerson and R.W. Vanderhaar *J.Chem.Phys.* **37** (1962) 2458
[164] F.H. Dorman and J.D. Morrison *J.Chem.Phys.* **35** (1961) 575
[165] C.P. Safvan, M. Krishnamurthy and D. Mathur *J. Phys. B.* **26** (1993) L837
[166] M. Mentinova and S.A. McLuckey *J. Am. Chem. Soc.* **132** (2010) 18248
[167] S.J. Pitteri and S.A. McLuckey *Mass Spec. Rev.* **24** (2005) 931
[168] A.H. Payne and G.L. Glish *Int. J. Mass Spectrom.* **204** (2001) 47
[169] D.K. Bohme *Phys.Chem.Chem.Phys.* **13** (2011) 18253
[170] L.A. Frank, W.R. Paterson, K.L. Ackerson, V.M. Vasyliunas, F.V. Coroniti and S.J. Bolton *Science* **274** (1996) 394
[171] S. Ghosh, K.K. Mahajan, J.M. Grebowsky and N. Nath *Journal of Geophysical Research-Space Physics* **100** (1995) 23983
[172] H.A. Taylor, H.C. Brinton, T.C.G. Wagner, B.H. Blackwell and G.R. Cordier *Ieee Transactions on Geoscience and Remote Sensing* **18** (1980) 44
[173] J.H. Hoffman, C.Y. Johnson, J.C. Holmes and J.M. Young *J. Geophys. Res.* **74** (1969) 6281
[174] E. Dubinin, R. Modolo, M. Fraenz, J. Woch, G. Chanteur, F. Duru, F. Akalin, D. Gurnett, R. Lundin, S. Barabash, J.D. Winningham, R. Frahm, J.J. Plaut and G. Picardi *Journal of Geophysical Research-Space Physics* **113** (2008) 16 A10217
[175] P.D. Feldman, D.F. Strobel, H.W. Moos and H.A. Weaver *Astrophys. J.* **601** (2004) 583
[176] J. Lilensten, O. Witasse, C. Simon, H. Solidi-Lose, O. Dutuit, R. Thissen and C. Alcaraz *Geophys. Res. Lett.* **32** (2005) L03203
[177] O. Witasse, O. Dutuit, J. Lilensten, R. Thissen, J. Zabka, C. Alcaraz, P.L. Blelly, S.W. Bougher, S. Engel, L.H. Andersen and K. Seiersen *Geophys. Res. Lett.* **29** (2002) 1263
[178] M. Alagia, N. Balucani, P. Candori, S. Falcinelli, F. Pirani, R. Richter, M. Rosi, S. Stranges and F. Vecchiocattivi *Rendiconti Lincei* **24** (2013) 53
[179] S. Falcinelli, F. Pirani, M. Alagia, L. Schio, R. Richter, S. Stranges, N. Balucani and F. Vecchiocattivi *Atmosphere* **7** (2016) Unsp 112
[180] S. Falcinelli, M. Rosi, P. Candori, F. Vecchiocattivi, J.M. Farrar, F. Pirani, N. Balucani, M. Alagia, R. Richter and S. Stranges *Planet Space Sci.* **99** (2014) 149
[181] J. Lilensten, C.S. Wedlund, M. Barthelemy, R. Thissen, D. Ehrenreich, G. Gronoff and O. Witasse *Icarus* **222** (2013) 169
[182] R. Linguerri, M. Hochlaf, M.C. Bacchus-Montabonel and M. Desouter-Lecomte *Phys.Chem.Chem.Phys.* **15** (2013) 824
[183] J.B. Hasted and A.Y.J. Chong *Proceedings of the Physical Society of London* **80** (1962) 441
[184] D.R. Bates and B.L. Moiseiwitsch *Proceedings of the Physical Society of London Section A* **67** (1954) 805
[185] A. Omont *Astron. Astrophys.* **164** (1986) 159
[186] T.J. Millar *Mon. Not. Roy. Astron. Soc.* **259** (1992) P35
[187] S. Leach *J. Electron. Spectrosc. Relat. Phenom.* **41** (1986) 427
[188] G. Javahery, S. Petrie, J. Wang and D.K. Bohme *Chem.Phys.Lett.* **195** (1992) 7
[189] S. Petrie and D.K. Bohme *Astrophys. J.* **540** (2000) 869
[190] S. Petrie, G. Javahery and D.K. Bohme *Astron. Astrophys.* **271** (1993) 662
[191] D.K. Bohme *Mass Spec. Rev.* **28** (2009) 672

[192] J. Roithova and D. Schroder *Phys.Chem.Chem.Phys.* **9** (2007) 2341
[193] C.L. Ricketts, D. Schroder, C. Alcaraz and J. Roithova *Chem-Eur.J.* **14** (2008) 4779
[194] E.E. Ferguson *Annu. Rev. Phys. Chem.* **26** (1975) 17

10. Required Permissions

Figure 1 Permission required from IoP

Figure 2 Maybe permission required from Elsevier, SDP article

Figure 3 Permission required from ACS. I can redraw and adapt this Figure if that is easier

Figure 4 Permission required from RSC publishing, SDP article

Figure 5 Permission required from RSC publishing, SDP article

Figure 6 Permission required from Elsevier, SDP article

Figure 7 Permission required from Elsevier

Figure 8 Permission required from Elsevier, SDP article

Figure 13 Permission required from Wiley.

Figure 14 Permission required from Elsevier, SDP article

Figure 15 Permission required from Wiley, SDP article.

Figure 16 Permission required from Wiley, SDP article.